Electronic Structure and Magnetic Properties of Solids

S. Y. Savrasov[a], A. Toropova[b],M. I. Katsnelson[c], A. I. Lichtenstein[d], V. Antropov[e], G. Kotliar[b]
[a] *Department of Physics, New Jersey Institute of Technology, Newark, NJ 07102, USA*
[b] *Department of Physics and Center for Material Theory, Rutgers University, Pscataway, NJ 08854, USA*
[c] *Department of Physics, University of Nijmegen, Nijmegen, The Netherlands*
[d] *Department of Physics, Hamburg University, Hamburg, Germany and*
[e] *Condensed Matter Physics Department, Ames Laboratory, Ames, IA 50011, USA*
(Dated: May 2003)

We review basic computational techniques for simulations of various magnetic properties of solids. Several applications to compute magnetic anisotropy energy, spin wave spectra, magnetic susceptibilities and temperature dependent magnetisations for a number of real systems are presented for illustrative purposes.

PACS numbers:

I. INTRODUCTION

This review covers main techniques and their applications developed in the past to calculate properties of magnetic systems by the methods of electronic structure theory of solids. The basic tool which was used in connections with these developments is a spin dependent version of density functional theory[1] which will be reviewed in Section II in its most general non–collinear form and including so called LDA+U method[2]. One of the oldest application of this method is the problem of magnetic anisotropy energy (MAE). Due to its technological relevance as well as the smallness of MAE, such calculations represent a real challenge to the theory and we review these efforts in Section III. In Section IV we address the problem of computing non–collinear spin alignments which is solved using an elegant spin spiral approach[3]. This allows us to simulate adiabatic spin dynamics of real magnets with relatively cheap computational effort, and some of the calculations will be discussed and compared to experiments. Another development which has been undertaken in the past is the direct calculation of exchange integrals by utilizing a formula of linear response theory[4]. This is reviewed in Section V. The spin waves, their dispersions and lifetimes as well as other spin fluctuations formally appear in the structure of dynamical spin susceptibility. The developments of electronic structure based on linear response approaches which access this quantity is reviewed in Section VI. The effect of electronic correlations are not small in the real materials and static mean field treatment done with local spin density functional or LSDA+U method may not be adequate for a whole range of solids. Bringing the effects of dynamical correlations to compute magnetic properties of real systems has been recently undertaken by utilizing the dynamical mean field theory[5]. This approach will be reviewed in Section VII together with some of its most recent applications. The reader is also refereed to several other reviews[6,7] on a similar subject as well as a few excellent books[8,9].

II. SPIN DENSITY FUNCTIONALS IN NON-COLLINEAR FORM

Here we describe a basic tool for computational studies of magnetic phenomena, a spin dependent version of the density functional theory[1]. We use general non–collinear notations and also treat the effects of spin –orbit coupling. We utilize local spin density approximation (LSDA) to the exchange–correlation functional and also show how the corrections due to strong electronic correlation effects appear in the functional in its simplest Hartree–Fock form known as the LDA+U method[2]. In section V we will also describe a more general first–principle method based on dynamical mean field theory[5] to include the correlation effects in a more rigorous manner.

To describe a magnetic solid we consider a system of fermions under an external potential V_{ext} and an external magnetic field $\mathbf{B}_{ext}$. It is useful to introduce the notion of the Kohn-Sham potential $V_{eff}(\mathbf{r})$ and the Kohn–Sham magnetic field $\mathbf{B}_{eff}(\mathbf{r})$. When spin–orbit coupling is present, the intra–atomic magnetization $\mathbf{m}(\mathbf{r})$ is not collinear, and the solid may choose different atom dependent quantization axes which makes magnetic moments pointing in different directions. Therefore, the magnetization must be treated as a general vector field, which also realizes non–collinear intra–atomic nature of this quantity. Such general magnetization scheme has been recently discussed[10]. In the non–collinear version of LSDA approach the total energy functional E is considered as a functional of two variables the charge density $\rho(\mathbf{r})$ and magnetization density $\mathbf{m}(\mathbf{r})$

$$\rho(\mathbf{r}) = \sum_{\mathbf{k}j} f_{\mathbf{k}j} \{ \vec{\psi}_{\mathbf{k}j}(\mathbf{r}) | \hat{I} | \vec{\psi}_{\mathbf{k}j}(\mathbf{r}) \} = \sum_{\mathbf{k}j} f_{\mathbf{k}j} \sum_{\sigma=\uparrow\downarrow} \psi^{(\sigma)*}_{\mathbf{k}j}(\mathbf{r}) \psi^{(\sigma)}_{\mathbf{k}j}(\mathbf{r}) \tag{1}$$

$$\mathbf{m}(\mathbf{r}) = g\mu_B \sum_{\mathbf{k}j} f_{\mathbf{k}j} \{\vec{\psi}_{\mathbf{k}j}(\mathbf{r})|\hat{\mathbf{s}}|\vec{\psi}_{\mathbf{k}j}(\mathbf{r})\} = g\mu_B \sum_{\mathbf{k}j} f_{\mathbf{k}j} \sum_{\sigma\sigma'=\uparrow\downarrow} \psi^{(\sigma)*}_{\mathbf{k}j}(\mathbf{r}) \hat{\mathbf{s}}_{\sigma\sigma'} \psi^{(\sigma')}_{\mathbf{k}j}(\mathbf{r}) \tag{2}$$

where $\{||\}$ denotes averaging over spin degrees of freedom only, the spin angular momentum operator is expressed in terms of Pauli matrices $\hat{\mathbf{s}} = \hat{\boldsymbol{\sigma}}/2$, $\hat{I}$ is 2×2 unit matrix, g is the gyromagnetic ratio which is for electrons equal to 2, and $\vec{\psi}_{\mathbf{k}j}(\mathbf{r})$ are the non–interacting Kohn–Sham particles are formally described by the two–component spinor wave functions

$$\vec{\psi}_{\mathbf{k}j}(\mathbf{r}) = \begin{pmatrix} \psi^{(\uparrow)}_{\mathbf{k}j}(\mathbf{r}) \\ \psi^{(\downarrow)}_{\mathbf{k}j}(\mathbf{r}) \end{pmatrix} \tag{3}$$

which define the charge and non–collinear magnetization densities of the electrons.

LSDA+U method[2] introduces additional variable "occupancy spin density matrix" $\hat{n}_{ab}$

$$\hat{n}_{ab} = \begin{pmatrix} n^{\uparrow\uparrow}_{ab} & n^{\uparrow\downarrow}_{ab} \\ n^{\downarrow\uparrow}_{ab} & n^{\downarrow\downarrow}_{ab} \end{pmatrix} \tag{4}$$

which represents the correlated part of electron density. To build up occupancy matrix one introduces a set of localized orbitals $\phi_a(\mathbf{r})$, associated with correlated electrons. Then

$$n^{\sigma\sigma'}_{ab} = \sum_{\mathbf{k}j} f(\epsilon_{\mathbf{k}j}) \langle \psi^{(\sigma)}_{\mathbf{k}j} | \phi_a \rangle \langle \phi_b | \psi^{(\sigma')}_{\mathbf{k}j} \rangle \tag{5}$$

The occupancy matrix becomes non-diagonal in spin space when spin–orbit coupling is taken into account. We include spin–orbit coupling in a variational way as suggested by Andersen[11].

One introduces a Lagrange multipliers matrix $\Delta\hat{V}_{ab}$ to enforce (5). The LSDA+U total energy functional is given by:

$$\begin{aligned} E[\rho(\mathbf{r}), \mathbf{m}(\mathbf{r}), \hat{n}_{ab}] &= \sum_{\mathbf{k}j} f(\epsilon_{\mathbf{k}j}) \epsilon_{\mathbf{k}j} - \int V_{eff}(\mathbf{r}) \rho(\mathbf{r}) d\mathbf{r} + \int \mathbf{B}_{eff}(\mathbf{r}) \mathbf{m}(\mathbf{r}) d\mathbf{r} - \sum_{ab} \sum_{\sigma\sigma'} \Delta V^{\sigma\sigma'}_{ab} n^{\sigma\sigma'}_{ab} \\ &+ \int V_{ext}(\mathbf{r}) \rho(\mathbf{r}) d\mathbf{r} - \int \mathbf{B}_{ext}(\mathbf{r}) \mathbf{m}(\mathbf{r}) d\mathbf{r} + \frac{1}{2} \int d\mathbf{r} d\mathbf{r}' \frac{\rho(\mathbf{r}) \rho(\mathbf{r}')}{|\mathbf{r} - \mathbf{r}'|} \\ &+ E^{LSDA}_{xc}[\rho, \mathbf{m}] + E^{Model}[\hat{n}_{ab}] - E^{Model}_{DC}[\hat{n}_{ab}]. \end{aligned} \tag{6}$$

The energies $\epsilon_{\mathbf{k}j}$ are determined by Pauli–like Kohn–Sham matrix equation:

$$[(-\nabla^2 + V_{eff})\hat{I} + g\mu_B \mathbf{B}_{eff} \hat{\mathbf{s}} + \xi \mathbf{l}\hat{\mathbf{s}} + \sum_{ab} \Delta\hat{V}_{ab} |\phi_a\rangle\langle\phi_b|] \, \vec{\psi}_{\mathbf{k}j} = \epsilon_{\mathbf{k}j} \, \vec{\psi}_{\mathbf{k}j} \tag{7}$$

Here $\hat{\mathbf{l}}$ and $\hat{\mathbf{s}}$ are one–electron orbital and spin angular momentum operator, respectively. $\xi(\mathbf{r})$ determines the strength of spin–orbit coupling and in practice is determined[12] by radial derivative of the $l = 0$ component of the Kohn–Sham potential inside an atomic sphere:

$$\xi(r) = \frac{2}{c^2} \frac{dV_{eff}(r)}{dr}. \tag{8}$$

$E^{LSDA}_{xc}[\rho, \mathbf{m}]$ is the LSDA exchange correlation energy. When magnetization is present, the exchange–correlation energy functional is assumed to be dependent on density and absolute value of the magnetization:

$$\begin{aligned} E^{LSDA}_{xc}[\rho, \mathbf{m}] &= \int d\mathbf{r} \epsilon_{xc}[\rho(\mathbf{r}), m(\mathbf{r})] \rho(\mathbf{r}) \\ &+ \int d\mathbf{r} f_{xc}[\rho(\mathbf{r}), m(\mathbf{r})] \; m(\mathbf{r}), \end{aligned} \tag{9}$$

where $m(\mathbf{r}) = |\mathbf{m}(\mathbf{r})|$.

$E^{Model}[\hat{n}_{ab}]$ is a contribution from the Coulomb energy in the shell of correlated electrons

$$E^{Model}[\hat{n}_{ab}] = \frac{1}{2}\sum_{\sigma}\sum_{abcd}\langle ac|v_C|bd\rangle n_{ab}^{\sigma\sigma} n_{cd}^{-\sigma-\sigma}$$
$$+\frac{1}{2}\sum_{\sigma}\sum_{abcd}(\langle ac|v_C|bd\rangle - \langle ac|v_C|db\rangle) n_{ab}^{\sigma\sigma} n_{cd}^{\sigma\sigma}$$
$$-\frac{1}{2}\sum_{\sigma}\sum_{abcd}\langle ac|v_C|db\rangle n_{ab}^{\sigma-\sigma} n_{cd}^{-\sigma\sigma} \tag{10}$$

This expression is nothing else as a Hartree–Fock average of the original expression for the Coulomb interaction

$$\frac{1}{2}\sum_{\sigma\sigma'}\sum_{abcd}\langle ab|v_C|cd\rangle c_{a\sigma}^{\dagger} c_{b\sigma'}^{\dagger} c_{d\sigma'} c_{c\sigma} \tag{11}$$

where the Coulomb interaction $v_C(\mathbf{r}-\mathbf{r}')$ has to take into account the effects of screening by conduction electrons. The matrix $\langle ac|v_C|bd\rangle = U_{abcd}$ is standardly expressed via the Slater integrals which for d–electrons are three constants $F^{(0)}, F^{(2)}$, and $F^{(4)}$ considered as the external parameters of the method. Its determination can for example be done using atomic spectral data, constrained density functional theory calculations or taken from spectroscopic experiments.

Since part of this Coulomb energy is already taken into account in LDA functional, the double–counting part denoted $E_{DC}^{Model}[\hat{n}_{ab}]$ must be subtracted. Frequently used form[2] for $E_{DC}^{Model}[\hat{n}_{ab}]$ is

$$E_{DC}^{Model}[\hat{n}_{ab}] = \frac{1}{2}\bar{U}\bar{n}(\bar{n}-1) - \frac{1}{2}\bar{J}[\bar{n}^{\uparrow}(\bar{n}^{\uparrow}-1) + \bar{n}^{\downarrow}(\bar{n}^{\downarrow}-1)] \tag{12}$$

where

$$\bar{U} = \frac{1}{(2l+1)^2}\sum_{ab}\langle ab|\frac{1}{r}|ab\rangle \tag{13}$$

$$\bar{J} = \bar{U} - \frac{1}{2l(2l+1)}\sum_{ab}(\langle ab|\frac{1}{r}|ab\rangle - \langle ab|\frac{1}{r}|ba\rangle) \tag{14}$$

and where $\bar{n}^{\sigma} = \sum_a n_{aa}^{\sigma\sigma}$ and $\bar{n} = \bar{n}^{\uparrow} + \bar{n}^{\downarrow}$.

The Kohn–Sham potential $V_{eff}(\mathbf{r})$ and Kohn–Sham magnetic field $\mathbf{B}_{eff}(\mathbf{r})$ are obtained by extremizing the functional with respect to $\rho(\mathbf{r})$ and $\mathbf{m}(\mathbf{r})$:

$$V_{eff}(\mathbf{r}) = V_{ext}(\mathbf{r}) + \int d\mathbf{r}'\frac{\rho(\mathbf{r}')}{|\mathbf{r}-\mathbf{r}'|} + \frac{\delta E_{xc}^{LSDA}[\rho,\mathbf{m}]}{\delta\rho(\mathbf{r})}, \tag{15}$$

$$\mathbf{B}_{eff}(\mathbf{r}) = \mathbf{B}_{ext}(\mathbf{r}) + \frac{\delta E_{xc}^{LSDA}[\rho,\mathbf{m}]}{\delta\mathbf{m}(\mathbf{r})}. \tag{16}$$

Extremizing with respect to $n_{ab}^{\sigma\sigma'}$ yield the correction to the potential $\Delta V_{ab}^{\sigma\sigma'}$

$$\Delta V_{ab}^{\sigma\sigma'} = \frac{dE^{Model}}{dn_{ab}^{\sigma\sigma'}} - \frac{dE_{DC}^{Model}}{dn_{ab}^{\sigma\sigma'}} \tag{17}$$

Then the spin diagonal elements for potential correction are given by:

$$\Delta V_{ab}^{\sigma\sigma} = \sum_{cd} U_{abcd} n_{cd}^{-\sigma-\sigma} + \sum_{cd}(U_{abcd} - U_{adcb}) n_{cd}^{\sigma\sigma}$$
$$-\delta_{ab}\bar{U}(\bar{n} - \frac{1}{2}) + \delta_{ab}\bar{J}(\bar{n}^{\sigma\sigma} - \frac{1}{2}), \tag{18}$$

and spin off–diagonal elements are given by

$$\Delta V_{ab}^{\sigma-\sigma} = -\sum_{cd} U_{adcb} n_{cd}^{-\sigma\sigma} \tag{19}$$

The off–diagonal elements of the potential correction only present when spin–orbit coupling is included, hence a relativistic effect.

This completes the description of the method and we now turn out to several applications of it.

III. MAGNETIC ANISOTROPY OF FERROMAGNETS

One of the oldest problems which has been addressed in the past is the calculation of the magneto–crystalline anisotropy energy (MAE)[13,14,15,16,17] of magnetic materials. The MAE is defined as the difference of total energies with the orientations of magnetization pointing in different, e.g., (001) and (111), crystalline axis. The difference is not zero because of spin–orbit effect, which couples the magnetization to the lattice, and determines the direction of magnetization, called the easy axis.

Being a ground state property, the MAE should be accessible in principle via spin density functional theory described above, and, despite the primary difficulty related to the smallness of MAE ($\sim 1\ \mu eV$/atom), great efforts to compute the quantity with advanced total energy methods combined with the development of faster computers, have seen success in predicting its correct orders of magnitudes [18,19,20,21,22]. However, the correct easy axis of Ni has not been predicted by the LSDA and a great amount of work has been done to understand what is the difficulty. These include (i) scaling spin–orbit coupling in order to enlarge its effect on the MAE[19,20], (ii) calculating torque to avoid comparing large numbers of energy[20], (iii) studying the effects of the second Hund's rule in the orbital polarization theory [21], (iv) analyzing possible changes in the position of the Fermi level by changing the number of valence electrons [22], (v) using the state tracking method[23], and (iv) real space approach[24].

It was recently suggested that the deficiency of the calculations is lying in improper treatment of the correlation effects and the intra–atomic repulsion U and exchange J should be taken into account. It is important to perform the calculations for fixed values of magnetic moments which themselves show some dependency on U and J as studied previously[25]. Since the pure LSDA result (U=0, and J=0) reproduces the experimental values for magnetic moments in both Fe and Ni fairly well, the $U-J$ parameter space should be scanned and the path of U and J values which hold the theoretical moments close to the experiment was extracted.

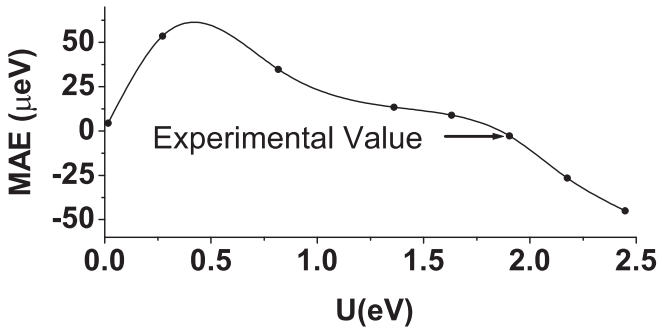

FIG. 1: The magneto–crystalline anisotropy energy MAE $= E(111) - E(001)$ for Ni as function of U. The experimental MAE is marked by arrow ($-2.8\ \mu eV$). The values of exchange parameter J for every value of U are chosen to hold the magnetic moment of 0.61 μ_B

The effect of correlations was found to be crucial in predicting the correct axis of Ni. Fig. 1 shows the results of this calculated MAE as a function of Coulomb parameter U. Walking along the path of parameters U and J which hold the magnetic moment to 0.6 μ_B the MAE first increases to 60 μeV ($U = 0.5\ eV$, $J = 0.3\ eV$) and then decreases. While decreasing it makes a rather flat area from $U = 1.4\ eV$, $J = 0.9\ eV$ to $U = 1.7\ eV$, $J = 1.1\ eV$ where MAE is positive and around 10 μeV. After the flat area, the MAE changes from the wrong easy axis to the correct easy axis. The correct magnetic anisotropy is predicted at $U = 1.9\ eV$ and $J = 1.2\ eV$. The change from the wrong easy axis to the correct easy axis occurs over the range of $\delta U \sim 0.2eV$, which is of the order of spin-orbit coupling constant ($\sim 0.1eV$).

For Fe (see Fig. 2), the MAE was calculated along the path of U and J values which fixes the magnetic moment to 2.2 μ_B. At $U = 0\ eV$ and $J = 0\ eV$, the MAE is 0.5 μeV. The correct MAE with the correct direction of magnetic moment is predicted at $U = 1.2\ eV$ and $J = 0.8\ eV$. It is remarkable that the values of U and J necessary to reproduce the correct magnetic anisotropy energy are very close to the values which are needed to describe photoemission spectra of these materials[26].

Recently, there has been a lot of experimental and theoretical studies devoted to CrO_2[27,28,29,30,31]. This compound has unusual half-metallic nature, it is a metal in one spin channel and an insulator in the other. CrO_2 demonstrates ferromagnetic ordering with magnetic moment $2\mu_b$ per Cr atom and Curie Temperature $T_C \simeq 390K$. A number of published works[27,28,29,30,31] addressed its band structure.

The results of the MAE computations within LSDA have been studied recently. Total energy calculations for three different directions [001], [010] and [102]. [001] axis indicate that easy magnetization axis within LSDA is

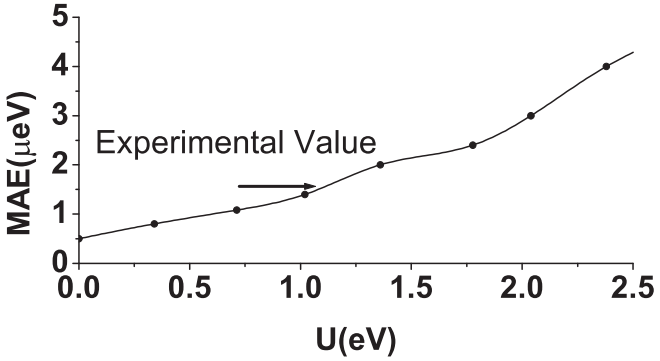

FIG. 2: The magneto–crystalline anisotropy energy MAE $= E(111) - E(001)$ for Fe as function of U. The experimental MAE is marked by arrow (1.4 μeV). The values of exchange parameter J for every value of U are chosen to hold the magnetic moment of $2.2\mu_B$

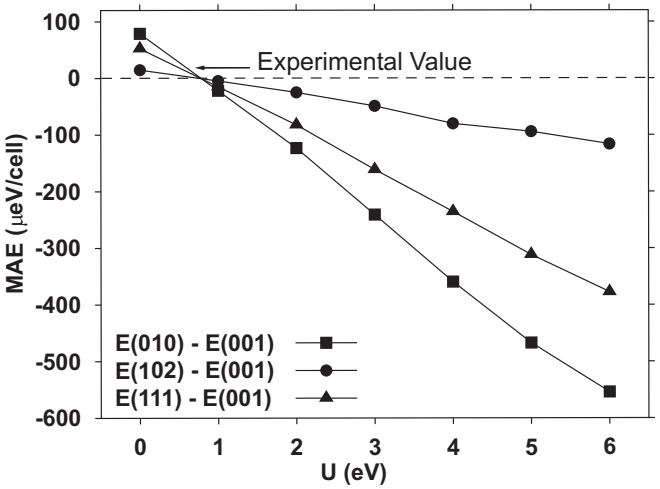

FIG. 3: The magneto–crystalline anisotropy energies MAE for CrO_2 as functions of U. The experimental value of MAE $E[010] - E[001] = 15.6\mu eV$ per cell is shown by arrow.

consistent with latest thin film experiments[33,34,35]. The numerical values of MAE however exceed the experimental one approximately two times.

In order to figure out the influence of intra-atomic repulsion U on the magnetic anisotropy, calculations have been also performed for finite value of U changing it from 0 to $6eV$ ($J = 0.87eV$ has been kept constant). These results are presented in Fig. 3. MAE is decreasing rapidly starting from LDA value $\approx 68\mu eV$ per cell and changes its sign around $U \approx 0.8eV$. This leads to switching of correct easy magnetization axis [001] to the wrong one, namely [102]. The biggest experimental value of MAE reported in the literature is $15.6\mu eV$ per cell[35]. The calculated MAE approaches this value around point $U = 0.6eV$. To summarize, the LSDA+U approach with $U \approx 0.6eV$ and $J = 0.87eV$ adequately describes the magneto–crystalline anisotropy of CrO_2.

We can conclude that the calculations of magnetic anisotropy energies in materials are only in its beginning stage of development .It is by now clear that the effects of Coulomb correlations must be taken seriously into account but the smallness of MAE and its sensitivity to the values of U used in the calculations prompts us that a predictive power of the method is yet to be achieved. More work is clearly required to develop robust algorithms calculating this highly important property of ferromagnets.

IV. SPIN SPIRAL METHOD AND FROZEN MAGNON CALCULATIONS

While ferromagnetic spin alignments are relatively simple to explore by the methods of spin density functional theory, the situation gets formally much more complicated when non–collinearity occurs. The simplest example of non–collinearity is the antiferromagnetism which is the ordering with wave-vector $\mathbf{q}$ corresponding to a zone–boundary

point of the Brillouin zone. This requires a choice of doubled unit cell so that in the new lattice this vector $\mathbf{q}$ becomes one of the reciprocal lattice vectors. In a more general sense we can consider an appearance of a spin spiral which gives orientation of different magnetic moments $\mathbf{M}_{\tau+R}$ for atoms of the sublattice $\boldsymbol{\tau}+\mathbf{R}$ ($\boldsymbol{\tau}$ is the basis vector, $\mathbf{R}$ is the primitive translation) in the form

$$\mathbf{M}_{\tau+R}=\left\{\begin{array}{c}M^x_{\tau+R}\\M^y_{\tau+R}\\M^z_{\tau+R}\end{array}\right\}=M_\tau\left\{\begin{array}{c}\cos(\mathbf{qR}+\phi_\tau)\sin(\theta_\tau)\\\sin(\mathbf{qR}+\phi_\tau)\sin(\theta_\tau)\\\cos(\theta_\tau)\end{array}\right\}, \tag{20}$$

where M_τ is the length of the atomic moment, and θ_τ, ϕ_τ are the angles describing its orientation in the unit cell with $\mathbf{R}=0$. As we see, in the systems with non–collinear ordering the situation gets immediately very complicated as for arbitrary $\mathbf{q}$ the size of the unit cell becomes prohibitively large. Note that here we do not assume that the size of the moment is varied when going from one cell to another. The latter is another type of so called incommensurate magnetism, the most known example of which is Cr.

Here we will briefly review a very elegant way to solve the problem of non–collinear magnetism where the size of the moment is kept constant which is known as the spin spiral method developed by Sandratski[7]. The problem when the size itself varies is more difficult one and the use of linear response theory will be discussed later of this review. The formal point is to note that non–collinear magnetic state destroys the periodicity of the original lattice and therefore the original Bloch theorem applied to the Kohn–Sham states $\vec{\psi}_{\mathbf{k}j}(\mathbf{r})$ is no longer available. However, the Bloch theorem in the present form reflects the translational symmetry properties of the lattice only it does not take into account the symmetry properties of the spin subsystem. A generalized symmetry treatment of the Hamiltonian for the non–collinear magnet can be developed. Let us define group operations acting on a spinor state $\vec{\psi}(\mathbf{r})$. These are (i) the translational operator $\hat{T}_R$ so that $\hat{T}_R\mathbf{r}=\mathbf{r}+\mathbf{R}$, (ii) the generalized rotation $\hat{g}$ which is a pure rotation $\hat{a}=(\alpha_g,\beta_g,\gamma_g)$ described by the 3x3 $j=1$ Wigner matrix $U^{j=1}_{mm'}(\alpha_g,\beta_g,\gamma_g)$ (where $\alpha_g,\beta_g,\gamma_g$ are the Euler angles) and possible shift by vector $\mathbf{b}$ for non–symmorphic group so that $\hat{g}\mathbf{r}=\hat{a}\mathbf{r}+\mathbf{b}$, (iii) the rotation $\hat{\xi}=(\alpha_\xi,\beta_\xi,\gamma_\xi)$ in the spin–$\frac{1}{2}$ subspace described by the 2x2 $j=\frac{1}{2}$ Wigner matrix $U^{j=1/2}_{\sigma\sigma'}(\alpha_\xi,\beta_\xi,\gamma_\xi)$.

The usefulness of these operations becomes immediately transparent if we explore symmetry properties of non–relativistic Hamiltonians $H_{\sigma\sigma'}(\mathbf{r})=(-\nabla^2+V_{eff})\delta_{\sigma\sigma'}+g\mu_B\mathbf{B}_{eff}\mathbf{s}_{\sigma\sigma'}$ of the type (7) with non–collinear spin alignments which assumes that the effective magnetic field $\mathbf{B}_{eff}$ inside each atom centered at $\boldsymbol{\tau}+\mathbf{R}$ transforms similar to (20). The translations $\mathbf{R}$ combined with the spin rotations $\hat{\xi}_{\{qR\tau\}}=(\theta_\tau,\mathbf{qR}+\phi_\tau,0)$ described by the unitary matrices $\hat{U}^{j=1/2}$ leave the spin spiral structure invariant. We thus arrive to a generalized Bloch theorem:

$$\vec{\psi}_{\mathbf{k}j}(\mathbf{r}+\mathbf{R})=e^{i\mathbf{kR}}\hat{U}^{j=1/2}(\theta_\tau,\mathbf{qR}+\phi_\tau,0)\vec{\psi}_{\mathbf{k}j}(\mathbf{r}) \tag{21}$$

Remarkably that this property allows us to restrict the consideration to a chemical unit cell and not to the supercell. Hence, instead of introducing the supercell whose size depends on the symmetry of wave vector $\mathbf{q}$, the non–collinear spin spiral states can still be treated with the Hamiltonians whose size does not depend on the wavevector $\mathbf{q}$.

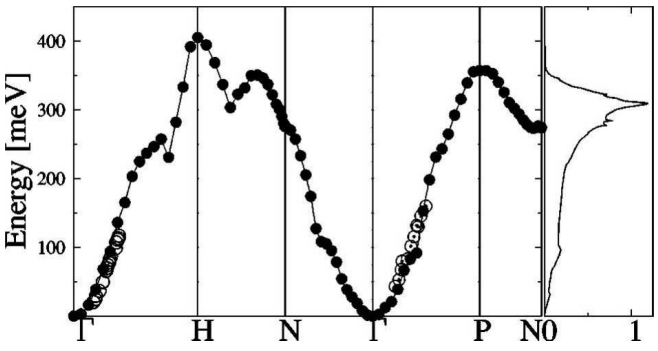

FIG. 4: Comparison between calculated using frozen magnon method and experimental[38] spin wave spectrum for Fe.

A variety of different calculations has been done with the spin spiral approach[6,7]. Halilov at. al[36,37] have studied adiabatic spin waves computed using a frozen magnon method. This is analogous to the frozen phonon method where atoms are displaced from their equilibrium positions and the total energy is restored as a function of these positions. Here the calculation is simplified since there is no necessity to introduce supercells, and can be performed for any general spin wave-vector $\mathbf{q}$. Fig. 4 reproduces the comparison between calculated using frozen magnon LSDA approach and experimental[38] spin wave spectra for Fe.

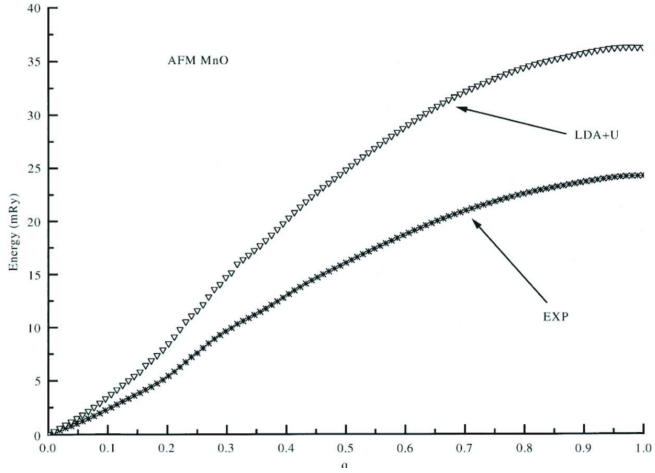

FIG. 5: Comparison between calculated using LDA+U method and experimental spin wave spectrum for NiO.

As we see the obtained agreement in these calculations is very satisfactory despite the fact that LSDA theory does not take into account important effects of dynamical correlations. For systems like NiO, the correlation effects become more important and the frozen magnon calculations using LSDA+U method have been carried out. Fig. 5 shows the comparison between calculated using LSDA+U method and experimental spin wave spectra for NiO. The overall agreement is good but important discrepancies remain which point out on the necessity to treat correlations effects among d–electrons beyond its simplest Hartree–Fock treatment as it is done within LSDA+U.

V. CALCULATIONS OF EXCHANGE CONSTANTS

While the density functional theory provide a rigorous description of the ground state properties of magnetic materials, the finite–temperature magnetism is estimated following a simple suggestion[4], whereby constrained DFT at $T = 0$ is used to extract exchange constants for a *classical* Heisenberg model, which in turn is solved using approximate methods (e.g. RPA, mean field) from a classical statistical mechanics of spin systems[4,36,39,40]. The recent implementation of this approach gives reasonable value of transition temperature for iron but not for nickel[41]. The analysis of exchange parameters for different classes of magnetic materials such as dilute magnetic semiconductors[42], molecular magnets[43], colossal magnetoresistance perovskites[44], transition metal alloys[45], hard magnetic materials such as PtCo[46] gives a useful information for magnetic simulations.

In this section we outline the general strategy for estimations of exchange interactions in solids. The most reliable way to consider spin excitations of itinerant electron magnets in the framework of the spin density functional approach is the use of frequency dependent magnetic susceptibility within the linear response theory[47,48,49].

$$\delta\mathbf{m} = \hat{\chi}\delta\mathbf{B}_{ext} = \hat{\chi}_0\delta\mathbf{B}_{eff}, \tag{22}$$

where χ_0 is a "bare" DFT and χ is an enhanced susceptibility. In collinear magnetic structures there are no coupling between the longitudinal and transverse components and for the transverse spin susceptibility we have the following equation:

$$\chi^{+-}(\mathbf{r},\mathbf{r}',\omega) = \chi_0^{+-}(\mathbf{r},\mathbf{r}',\omega) + \int d\mathbf{r}''\chi_0^{+-}(\mathbf{r},\mathbf{r}'',\omega)I(\mathbf{r}'')\chi^{+-}(\mathbf{r}'',\mathbf{r}',\omega) \tag{23}$$

where $I = B_{xc}/m$ is an exchange-correlation "Hund's rule" interaction. This random–phase–approximation (RPA) like equation is formally exact in the adiabatic time dependent version of density functional theory (TD–DFT)[50]. The bare susceptibility has the following form:

$$\chi_0^{+-}(\mathbf{r},\mathbf{r}',\omega) = \sum_{\mu\nu}\frac{f_{\mu\uparrow} - f_{\nu\downarrow}}{\omega - \varepsilon_{\mu\uparrow} + \varepsilon_{\nu\downarrow}}\psi^*_{\mu\uparrow}(\mathbf{r})\psi_{\nu\downarrow}(\mathbf{r})\psi^*_{\nu\downarrow}(\mathbf{r}')\psi_{\mu\uparrow}(\mathbf{r}') \tag{24}$$

where $\psi_{\mu\sigma}$ and $\varepsilon_{\mu\sigma}$ are eigenstates and eigenvalues for the Kohn–Sham quasiparticles. We can rewrite the equation for the transverse susceptibility as

$$\widehat{\chi}^{+-} = \left(m + \widehat{\Lambda}\right)\left(\omega - I_{xc}\widehat{\Lambda}\right)^{-1} \tag{25}$$

where

$$\Lambda(\mathbf{r},\mathbf{r}',\omega) = \sum_{\mu\nu}\frac{f_{\mu\uparrow} - f_{\nu\downarrow}}{\omega - \varepsilon_{\mu\uparrow} + \varepsilon_{\nu\downarrow}}\psi^*_{\mu\uparrow}(\mathbf{r})\psi_{\nu\downarrow}(\mathbf{r})\nabla\left[\psi_{\mu\uparrow}(\mathbf{r}')\nabla\psi^*_{\nu\downarrow}(\mathbf{r}') - \psi^*_{\nu\downarrow}(\mathbf{r}')\nabla\psi_{\mu\uparrow}(\mathbf{r}')\right] \tag{26}$$

Spin wave excitations can be separated from the Stoner continuum (e.g., paramagnons) only in the adiabatic approximation, which means the replacement $\Lambda(\mathbf{r},\mathbf{r}',\omega)$ by $\Lambda(\mathbf{r},\mathbf{r}',0)$ in Eq.(25). Otherwise one should just find the poles of the total susceptibility, and the whole concept of "exchange interactions" is not uniquely defined. Nevertheless, *formally* we can introduce the effective exchange interactions via the quantities

$$\Omega(\mathbf{r},\mathbf{r}',\omega) = I_{xc}\Lambda(\mathbf{r},\mathbf{r}',\omega). \tag{27}$$

In the static limit one can show that

$$\Omega(\mathbf{r},\mathbf{r}',0) = \frac{1}{m(\mathbf{r})}J(\mathbf{r},\mathbf{r}',0) - B_{xc}(\mathbf{r})\boldsymbol{\delta}(\mathbf{r}-\mathbf{r}') \tag{28}$$

where an expression for frequency dependent exchange interactions has the following form

$$J(\mathbf{r},\mathbf{r}',\omega) = \sum_{\mu\nu}\frac{f_{\mu\uparrow} - f_{\nu\downarrow}}{\omega - \varepsilon_{\mu\uparrow} + \varepsilon_{\nu\downarrow}}\psi^*_{\mu\uparrow}(\mathbf{r})B_{xc}(\mathbf{r})\psi_{\nu\downarrow}(\mathbf{r})\psi^*_{\nu\downarrow}(\mathbf{r}')B_{xc}(\mathbf{r}')\psi_{\mu\uparrow}(\mathbf{r}') \tag{29}$$

The later coincides with the exchange integrals[4,6] if we neglect the ω - dependence. Since $B_{xc} \sim m$ we have $J \sim m^2$ and the expression (27) vanishes in non-magnetic case, as it should be. Note that the static susceptibility $\widehat{\chi}^{+-}(\omega = 0)$ can be represented in the following form

$$\widehat{\chi}^{+-}(0) = m\left(\widehat{\Omega}^{-1} - B_{xc}^{-1}\right) \equiv m\widehat{\widehat{\Omega}} \tag{30}$$

which is equivalent to the result of Ref.[51]

$$\widehat{\widehat{\Omega}} = \widehat{\Omega}\left(1 - B_{xc}^{-1}\widehat{\Omega}\right)^{-1} \tag{31}$$

for the renormalized exchange interaction if one define them in terms of inverse *static* susceptibility[52]. Note, that the magnon frequencies are just eigenstates of the operator $\widehat{\Omega}(0)$ which exactly corresponds to the expression from the unrenormalized exchange interactions[4,6]. Note that for the long-wavelength limit $\mathbf{q} \to 0$ this result turns out to be exact which proves the above statement about the stiffness constant D: in the framework of the local approximation it is rigorous.

Let us compare the Eq.31 with the Heisenberg–like dispersion law in the spherical approximation for the spin-wave spectrum in terms of static transverse susceptibility[6]:

$$\omega_{\mathbf{q}} = m\left[\chi_{\mathbf{q}}^{-1} - \chi_0^{-1}\right]. \tag{32}$$

Now we will use an expression $\widehat{J} = \widehat{\chi}^{-1}$which gives the well–known connection between the inverse static susceptibility and the parameter Φ_2 in the Landau theory of phase transitions. To analyze the relationship between the dispersion law (32) and that commonly used in the DFT, $\omega^l_{\mathbf{q}} = mI\left[\chi_0 - \chi_{\mathbf{q}}\right]I$, we assume that the ratio

$$\Delta_{\mathbf{q}} = \left(\chi_{\mathbf{q}} - \chi_0\right)\chi_0^{-1} \approx \omega^l_{\mathbf{q}}/mI \tag{33}$$

is small in the long-wave approximation. Then, by expanding Eq.32 over the parameter $\Delta_{\mathbf{q}}$, we obtain the desired result:

$$\begin{aligned}\omega_{\mathbf{q}} &= m\left(\chi_{\mathbf{q}}^{-1} - \chi_0^{-1}\right) = m\chi_0^{-1}\Delta_{\mathbf{q}}\left(1 - \Delta_{\mathbf{q}}\right)^{-1} \\ &\simeq m\chi_0^{-1}\left(\chi_0 - \chi_{\mathbf{q}}\right)\chi_0^{-1} = m\left(J_0^l - J_{\mathbf{q}}^l\right)\end{aligned} \tag{34}$$

or

$$J_{\mathbf{q}} = J_0 \left[1 + \Delta_{\mathbf{q}} \left(1 - \Delta_{\mathbf{q}}\right)^{-1}\right] = J_0 \left[1 + \Delta_{\mathbf{q}} + \Delta_{\mathbf{q}}^2 + ..\right], \tag{35}$$

where the susceptibility has a matrix structure and

$$J_{\mathbf{q}}^l = J_0 \left(1 + \Delta_{\mathbf{q}}\right) = \chi_0^{-1} \chi_{\mathbf{q}} \chi_0^{-1} = I \chi_{\mathbf{q}} I \tag{36}$$

is the matrix of the exchange parameter in the local (long–wave) approximation. We take into account, that in the ferromagnetic state $\chi_0^{-1} = I$. A form of Eq.(36) is the widely accepted definition of the exchange coupling parameter. The usual assumption of weak enhancement $J_{\mathbf{q}} - J_0 = J_{\mathbf{q}}^0 - J_0^0$ is valid due to the well–known result $\chi_{\mathbf{q}}^{-1} = J_{\mathbf{q}} = J_{\mathbf{q}}^0 - I$. As a consequence, the spectrum of elementary excitations is not affected by exchange–correlation enhancement effects in linear response regime. So, the definition (36) is directly related to several very strong approximations: rigid spin, smallness of spin wave dispersion compared to the effective exchange splitting (atomic limit).

Below we will briefly mention calculations of the exchange parameters and adiabatic spin wave spectra using the multiple scattering technique in the local density approximation with a linear muffin–tin orbital technique (LMTO) in the atomic sphere approximation[11]. Three ferromagnetic systems with entirely different degree of localization of the local moment were considered: Gd, Ni and Fe[6]. An important observation is that in Gd (highly localized moments, small spin wave dispersion) the approximation based on the assumption $\Delta_{\mathbf{q}} << 1$ is completely fulfilled (Δ at the zone boundary is less then 0.01), whereas in Ni (moderately localized moments, large spin wave dispersion) it is not valid at all ($\Delta \simeq 0.6$ at $\mathbf{q} = Y$), so that the corresponding matrix estimates using Eq.(34) demonstrate a strong enhancement of spin wave spectra at larger $\mathbf{q}$. Fe is an intermediate case where the maximum of Δ is 0.30.

Practical expression for the exchange coupling has been derived[52] using multiple scattering method:

$$J_{\mathbf{q}}^{+-} = \frac{1}{4\pi} \int^{\varepsilon_F} d\varepsilon Im \mathrm{Tr}_L \left(T^{\uparrow} - T^{\downarrow}\right)_{00} \left[\int d\mathbf{k} T_{\mathbf{k}}^{\uparrow} T_{\mathbf{k}+\mathbf{q}}^{\downarrow}\right]^{-1} \left(T^{\uparrow} - T^{\downarrow}\right)_{00}. \tag{37}$$

where T^{σ} is a path operator. This expression properly takes into account both exchange effects related to the Stoner splitting and the different energy dispersion for different spins in band magnets.

Analysis of the effective exchange coupling between atoms after Eq. (37) indicated that in Fe and Ni the main contribution came from the renormalization of the first nearest neighbor exchange, so that in bcc Fe it is increased from J_{01}^l=16.6 meV to J_{01}=19.4 meV, whereas in fcc Ni J_{01}^l=2.7 meV to J_{01}=8.3 meV. Such a clear difference in the results indicates that the removal of the long–wave approximation can serve as an indicator of the degree of localization (parameter $\left(\chi_{\mathbf{q}} - \chi_0\right) \chi_0^{-1}$ above) in different metallic magnets. In Fe and Ni, for instance, it at least partially explains why long wavelength mean field estimates predict such a small T_c in FM Ni: 300–350K in Ref.[6], 340 K in present calculations, while experimental result is 630 K. First of all, long–wave approximation is suitable for such a 'localized' system as Fe, and the corresponding change in the nearest neighbor J_{01} is relatively small (correspondingly the increase of T_c is expected to be small). Ferromagnetic Ni represents a rather itinerant system and any local approach (long wave approximation in particular) might produce a large error. Also in Ni at T_c the energy associated with 'creation' of moment is comparable with the energy of its rotation and longitudinal fluctuations should be taken into account.

A large increase in J_{01} for Ni may indicate that traditional mean–field approaches (based on the absence of short–range order) are not applicable for the itinerant systems in general, predicting very high T_c (above 1000K). Such a number is not consistent with the local density approach because the latter does not allow to have T_c in fcc Ni larger then 500-540K (600-640K using gradient corrections) and this number can be considered only as an indicator of non–applicability of mean field approach.

VI. DYNAMICAL SPIN SUSCEPTIBILITY CALCULATIONS

Local spin density functional theory and the LDA+U method have been applied with success to study full wave–vector and frequency dependent spin susceptibility χ of solids. Its knowledge accessible directly via neutron–scattering measurements is important due to significant influence of spin fluctuations to many physical properties and phenomena[8], such, *e.g.*, as the electronic specific heat, electrical and thermal resistivity, suppression of superconductivity for singlet spin pairing, *etc* . As we already discussed, in magnetically ordered materials, transverse spin fluctuations are spin waves whose energies and lifetimes are seen in the structure of transverse susceptibility.

Large efforts in the past were put on the development of methods for *ab initio* calculations of the dynamical spin susceptibility based either on the random–phase–approximation (RPA) decoupling of the Bethe–Salpeter equation[53], or within density functional formalism[54]. Quantitative estimates of χ with realistic energy bands, wave functions, and

self–consistently screened electron–electron matrix elements appeared in the literature more than 3 decades ago[48,55,56]. More recently, a computationally efficient time–dependent generalization of the Sternheimer approach[57] originally developed for *ab initio* calculations of phonon dispersions, electron–phonon interactions and transport properties of transition–metal materials has been proposed[49].

This method is advantageous since it allows us to avoid problems connected to the summations over higher energy states and inversions of large matrices. It considers the response of electrons to a small external magnetic field

$$\delta\mathbf{B}_{ext}(\mathbf{r}t) = \delta\mathbf{b}e^{i(\mathbf{q}+\mathbf{G})\mathbf{r}}e^{i\omega t}e^{-\eta|t|} + c.c \tag{38}$$

applied to a solid. Here $\delta\mathbf{b} = \sum_\mu \delta b^\mu \mathbf{e}_\mu$ shows a polarization of the field (μ runs over x, y, z or over $-1, 0, 1$), wave vector $\mathbf{q}$ lies in the first Brillouin zone, $\mathbf{G}$ is a reciprocal lattice vector, and η is an infinitesimal positive quantity. If the unperturbed system is described by charge density $\rho(\mathbf{r})$ and by magnetization $\mathbf{m}(\mathbf{r})$, the main problem is to find self–consistently first–order changes $\delta\rho(\mathbf{r}t)$ and $\delta\mathbf{m}(\mathbf{r}t) = \sum_\nu \delta m_\nu(\mathbf{r}t)\mathbf{e}^\nu$ induced by the field $\delta\mathbf{B}_{ext}(\mathbf{r}t)$. If the polarization $\delta\mathbf{b}$ in (38) is fixed to a particular μth direction, and $\delta\mathbf{m}(\mathbf{r}t)$ is calculated afterwards, a μth column of the spin susceptibility matrix $\chi_{\nu\mu}(\mathbf{r}, \mathbf{q}+\mathbf{G}, \omega)$ will be found.

Employment of *time–dependent* (TD) version of density functional theory (DFT)[50] to find the quantities $\delta\rho(\mathbf{r}t)$ and $\delta\mathbf{m}(\mathbf{r}t)$ can be useful because in order to find the dynamical response within TD DFT, only the knowledge of these unperturbed Kohn–Sham states (both occupied and unoccupied) is required; no knowledge of real excitation spectra (both energies and lifetimes) is necessary. This is the main advantage of such approach. Unfortunately, within TD DFT, an accurate approximation to the kernel $I_{xc}(\mathbf{r}, \mathbf{r}', \omega)$ describing dynamical exchange–correlation effects is unknown while some progress is currently been made[58]. In the past, the so called adiabatic local density approximation (ALDA)[50] and a generalized gradient approximation[60] (GGA) are adopted to treat $I_{xc}(\mathbf{r}, \mathbf{r}', \omega)$. The addition of the local U corrections has been addressed in the work[59].

One can develop a *variational* linear–response formulation. It has already been known that *static* charge and spin susceptibilities appeared as second–order changes in the total energy due to applied external fields can be calculated in a variational way. This was demonstrated long time ago[61] on the example of magnetic response, and, recently[57,62], in the problem of lattice dynamics which is an example of charge response. The proof is directly related to a powerful "$2n+1$" theorem of perturbation theory and stationarity property for the total energy itself[63]. Any $(2n+1)$th change in the total energy E_{tot} involves finding only (n)th order changes in one–electron wave functions ψ_i, and corresponding changes in the charge density as well as in the magnetization. Any $(2n)$th change in E_{tot} is then variational with respect to the (n)th–order changes in ψ_i.

A time–dependent generalization of these results was addressed[49], where the action S as a functional of $\rho(\mathbf{r}t)$ and $\mathbf{m}(\mathbf{r}t)$ is considered within TD DFT[50,64]. These functions are expressed via Kohn–Sham spinor orbitals $\vec{\psi}_{\mathbf{k}j}(\mathbf{r}t)$ satisfying TD Schrödinger's equation. Therefore, S as the stationary functional of $\vec{\psi}_{\mathbf{k}j}(\mathbf{r}t)$ is considered in practice. When the external field is small, the perturbed wave function is represented as $\vec{\psi}_{\mathbf{k}j}(\mathbf{r})\, e^{-i\epsilon_{\mathbf{k}j}t} + \delta\vec{\psi}_i(\mathbf{r}t)$ and the first–order changes $\delta\vec{\psi}_{\mathbf{k}j}(\mathbf{r}t)$ define the induced charge density as well as the magnetization:

$$\delta\rho = \sum_{\mathbf{k}j}\left(\{\delta\vec{\psi}_{\mathbf{k}j}|I|\vec{\psi}_{\mathbf{k}j}\} + \{\vec{\psi}_{\mathbf{k}j}|I|\delta\vec{\psi}_{\mathbf{k}j}\}\right) \tag{39}$$

$$\delta\mathbf{m} = g\mu_B\sum_i\left(\{\delta\vec{\psi}_{\mathbf{k}j}|\hat{\mathbf{s}}|\vec{\psi}_{\mathbf{k}j}\} + \{\vec{\psi}_{\mathbf{k}j}|\hat{\mathbf{s}}|\delta\vec{\psi}_{\mathbf{k}j}\}\right) \tag{40}$$

In order to find $\delta\vec{\psi}_{\mathbf{k}j}(\mathbf{r}t)$, a time–dependent analog of the "$2n+1$" theorem is now introduced. Any $(2n+1)$th change in the action functional S involves finding only (n)th order changes in the TD functions $\vec{\psi}_{\mathbf{k}j}(\mathbf{r}t)$, and corresponding changes in charge density as well as in the magnetization. Any $(2n)$th change in S is then variational with respect to the (n)th–order changes in $\vec{\psi}_{\mathbf{k}j}(\mathbf{r}t)$. The proof is the same as for the static case[63] if the stationarity property of S and the standard TD perturbation theory are exploited. For important case $n = 2$, this theorem makes the second–order change $S^{(2)}$ in the action *variational* with respect to the first–order changes $\delta\vec{\psi}_i(\mathbf{r}t)$. If the perturbation has the form (38), $S^{(2)}$ is directly related to the real diagonal part of the dynamical spin susceptibility $Re[\chi_{\nu\mu}(\mathbf{q}+\mathbf{G}', \mathbf{q}+\mathbf{G}, \omega)]_{\mathbf{G}'=\mathbf{G}}$, thus allowing its variational estimate[64].

The problem is now reduced to find $S^{(2)}$ as a functional of $\delta\vec{\psi}_{\mathbf{k}j}(\mathbf{r}t)$ and to minimize it. This will bring an equation for $\delta\vec{\psi}_{\mathbf{k}j}(\mathbf{r}t)$. Any change in the action functional can be established by straightforward varying S of TD DFT[50,64] with respect to the perturbation (38). This is analogous to what is done in the static DFT to derive, for example,

the dynamical matrix[57]. $S^{(2)}$ is found to be

$$S^{(2)}[\delta\vec{\psi}_{\mathbf{k}j}] = \sum_{\mathbf{k}j} 2\left\langle \delta\vec{\psi}_{\mathbf{k}j}\,|H - i\partial_{\mathbf{k}j} I|\,\delta\vec{\psi}_{\mathbf{k}j}\right\rangle + \int \delta\rho\delta V_{eff} - \int \delta\mathbf{m}(\delta\mathbf{B}_{eff} + \delta\mathbf{B}_{ext}) \tag{41}$$

where the unperturbed 2×2 Hamiltonian matrix $\hat{H} = (-\nabla^2 + V_{eff})\hat{I} - g\mu_B \hat{\mathbf{s}}\mathbf{B}_{eff} + \xi\mathbf{l}\hat{\mathbf{s}}$. δV_{eff} and $\delta\mathbf{B}_{eff}$ are their first–order changes induced by the perturbation (38) which involve the Hartree (for δV_{eff}) and the exchange–correlation contributions expressed via $\delta\rho$ and $\delta\mathbf{m}$ in the standard manner[54].

The differential equation for $\delta\vec{\psi}_{\mathbf{k}j}\,(\mathbf{r}t)$ derived from the stationarity condition of (41) is given by

$$(H - i\partial_{\mathbf{k}j}\hat{I})\delta\vec{\psi}_{\mathbf{k}j} + (\delta V_{eff}\hat{I} - \mu_B\boldsymbol{\sigma}\delta\mathbf{B}_{eff})\vec{\psi}_{\mathbf{k}j} = 0 \tag{42}$$

Applications to transverse spin fluctuations in Fe and Ni as well as calculations of paramagnetic response in Cr and Pd have demonstrated an efficiency of the approach. Experimental evidence of an "optical" spin–wave branch for Ni[65] and its absence for Fe[38] was correctly described . The dynamical susceptibility was calculated *ab initio* for paramagnetic Cr, a highly interesting material due to its incommensurate antiferromagnetism[66]. The calculation predicted a wave vector of the spin density wave (SDW), and clarified the role of Fermi–surface nesting. Strong long–wavelength spin fluctuations of Pd were evident from these and earlier[56] theoretical studies.

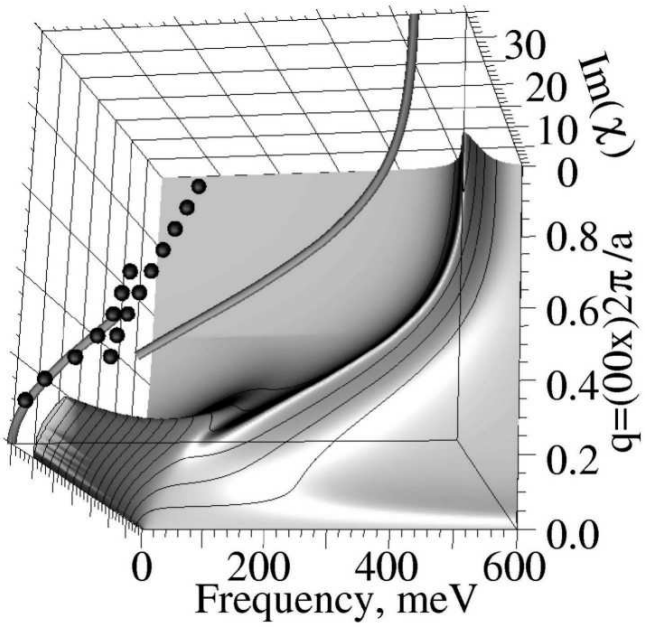

FIG. 6: Calculated $Im[\chi_{+-}(\mathbf{q},\omega)]$ (arb.units) for Ni. Experimental data[65] are indicated by balls.

We reproduce some of the calculations at Fig. 6 and Fig. 7 which show calculated $Im[\chi(\mathbf{q},\omega)]$ for ferromagnetic Ni and paramagnetic bcc Cr. In particular, for Cr, a remarkable structure is clearly seen for the $\mathbf{q}'$s near $(0,0,x_{SDW}\sim 0.9)2\pi/a$, where the susceptibility is mostly enhanced at low frequencies. This predicts Cr to be an incommensurate antiferromagnet (experimentally, x_{SDW}=0.95).

A scheme for making *ab initio* calculations of the dynamic paramagnetic spin susceptibilities of solids at finite temperatures was recently described[67] where incommensurate and commensurate antiferromagnetic spin fluctuations in paramagnetic Cr and compositionally disordered $Cr_{95}V_5$ and $Cr_{95}Re_5$ alloys were studied together with the connection with the nesting of their Fermi surfaces.

To conclude, the developed approach is able to describe known spin–fluctuational spectra of some real materials which demonstrated its efficiency for practical *ab initio* calculations. however, more elaborate approximations to the dynamical exchange and correlation are clearly required in order to account for the observed discrepancies. The next section discussed a more general framework to deal with the correlation effects.

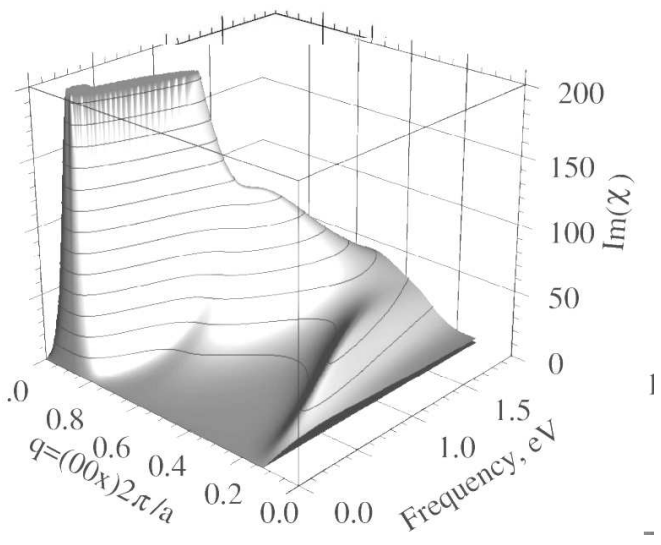

FIG. 7: Calculated $Im[\chi_{+-}(\mathbf{q},\omega)]$ (Ry^{-1}) for Cr.

VII. DYNAMICAL MEAN FIELD APPROACH AND THE REGIME OF STRONG CORRELATIONS

Magnetic materials range from very weak having a small magnetization to strong ones which exhibit a saturated magnetization close to the atomic value. As we have seen in the previous sections, frequently, weak or itinerant magnets are well described by spin density wave theory, where spin fluctuations are localized in a small region of momentum space. Quantitatively they are well described by LSDA. The transition from ordered to paramagnetic state is driven by amplitude fluctuations. In strong magnets, there is a separation of time scales, $\hbar/t$ is the time scale for an electron to hop from site to site with hopping integral t, which is much shorter than $\hbar/J$, the time scale for the moment to flip in the paramagnetic state. The spin fluctuations are localized in real space and the transition to the paramagnetic state is driven by orientation fluctuations of the spin. The exchange splitting J is much larger than the critical temperature.

Obtaining a quantitative theory of magnetic materials valid both in weak and in strong coupling, above and below the critical temperature has been a theoretical challenge for many years. It has been particularly difficult to describe the regime above T_c in strong magnets when the moments are well formed but their orientation fluctuates. This problem, for example, arises in magnetic insulators above their ordering temperature, when this ordering temperature is small compared to electronic scales, a situation that arises in transition metal monoxides (NiO and MnO) and led to the concept of a Mott insulator. In these materials the insulating gap is much larger than the Néel temperature. Above the ordering temperature, we have a collection of atoms with an open shell interacting via superexchange. This is a local moment regime which cannot be accessed easily with traditional electronic structure methods.

Two important approaches were designed to access the disordered local moment (DLM) regime. One approach[68] starts form a Hubbard like Hamiltonian and introduces spin fluctuations via the Hubbard–Stratonovich transformation[69,70,71,72] which is then evaluated using a static coherent potential approximation (CPA) and improvements of this technique. A dynamical CPA[73] was developed by Kakehashi[74]. A second approach begins with solutions of the Kohn–Sham equations of a constrained LDA approximation in which the local moments point in random directions, and averages over their orientation using the KKR–CPA approach[75,76]. The average of the Kohn–Sham Green functions then can be taken as the first approximation to the true Green functions, and information about angle resolved photoemission spectra can be extracted[77,78]. There are approaches that are based on a picture where there is no short range order to large degree. The opposite point of view, where the spin fluctuations far away form the critical temperature are still relatively long ranged was put forward in the fluctuation local band picture[79,80,81].

Description of the behavior near the critical point requires renormalization group methods, and the low temperature treatment of this problem is still a subject of intensive research[82]. There is also a large literature on describing magnetic metals using more standard many–body methods[83,84,85,86,87].

Dynamical mean field theory (DMFT) can be used to improve treatment to include dynamical fluctuations beyond static approximations like LSDA or LSDA+U. This is needed to get access to disordered local moment regime and beyond. Notice that single site DMFT includes some degree of short range correlations. Cluster methods can be used to go beyond the single site DMFT to improve the description of short range order on the quasiparticle spectrum.

DMFT also allows us to incorporate the effects of the electron–electron interaction on the electronic degrees of freedom. This is relatively important in metallic systems such as Fe and Ni and absolutely essential to obtain the Mott–Hubbard gap in transition metal monoxides.

Realistic implementation of DMFT within electronic structure framework[88,89] can be viewed as a spectral density functional theory[90,91,92,93]. The central quantity of this method is the local Green function $\hat{G}_{loc}(\mathbf{r},\mathbf{r}',\omega)$, which in the non–collinear version should be considered as the matrix in spin variables

$$\hat{G}_{loc} = \begin{pmatrix} G^{\uparrow\uparrow} & G^{\uparrow\downarrow} \\ G^{\downarrow\uparrow} & G^{\downarrow\downarrow} \end{pmatrix} \tag{43}$$

The local Green function is only a part of the full one–electron Green function restricted which is restricted within a certain cluster area. Due to translational invariance of the Green function on the original lattice given by primitive translations $\{\mathbf{R}\}$, i.e. $\hat{G}(\mathbf{r}+\mathbf{R},\mathbf{r}'+\mathbf{R},\omega) = \hat{G}(\mathbf{r},\mathbf{r}',\omega)$, it is always sufficient to consider $\mathbf{r}$ lying within a primitive unit cell Ω_c positioned at $\mathbf{R}=0$. Thus, $\mathbf{r}'$ travels within some area Ω_{loc} centered at $\mathbf{R}=\mathbf{0}$. We therefore define the local Green function to be the exact Green function $G(\mathbf{r},\mathbf{r}',z)$ within a given cluster Ω_{loc} and zero outside. In other words,

$$\hat{G}_{loc}(\mathbf{r},\mathbf{r}',\omega) = \hat{G}(\mathbf{r},\mathbf{r}',\omega)\theta_{loc}(\mathbf{r},\mathbf{r}') \tag{44}$$

where the theta function is a unity when vector $\mathbf{r}\in\Omega_c, \mathbf{r}'\in\Omega_{loc}$ and zero otherwise. A functional theory where the total free energy of the system Γ_{SDF} considers the local Green function as a variable was developed recently[90,91,92,93]. It is more powerful than the ordinary DFT since it accesses both the energetics and local excitational spectra of real materials. The range of locality is in principle our choice and the theory has a correct scaling in predicting full $\mathbf{k}$– and ω dependent spectrum of excitations when this range is expanded till infinity. If the range is collapsed to a single site, only the density of states is predicted.

A numerically tractable approach was developed completely similar to the density functional theory with the introduction of energy–dependent analog of Kohn–Sham orbitals. They are very helpful to write down the kinetic energy portion of the functional similar to as DFT considers the density functional as the functional of Kohn–Sham wave functions. It is first useful to introduce the notion of an local self–energy operator

$$\begin{aligned} \mathcal{M}^{\sigma\sigma'}_{eff}(\mathbf{r},\mathbf{r}',\omega) &= V_{ext}(\mathbf{r})\delta(\mathbf{r}-\mathbf{r}')\delta_{\sigma\sigma'} + \mathcal{M}^{\sigma\sigma'}_{int}(\mathbf{r},\mathbf{r}',\omega) \\ &= [V_{ext}(\mathbf{r}) + V_H(\mathbf{r})]\delta(\mathbf{r}-\mathbf{r}')\delta_{\sigma\sigma'} + \mathcal{M}^{\sigma\sigma'}_{xc}(\mathbf{r},\mathbf{r}',\omega) \end{aligned}$$

which has the same range of locality as the local Green function. Second, an auxiliary Green function $\mathcal{G}^{\sigma\sigma'}(\mathbf{r},\mathbf{r}',i\omega)$ connected to our new "interacting Kohn–Sham" particles so that it is defined in the entire space by the relationship

$$[\mathcal{G}^{-1}]^{\sigma\sigma'}(\mathbf{r},\mathbf{r}',\omega) = [G_0^{-1}]^{\sigma\sigma'}(\mathbf{r},\mathbf{r}',\omega) - \mathcal{M}^{\sigma\sigma'}_{int}(\mathbf{r},\mathbf{r}',\omega).$$

where $G_0^{\sigma\sigma'}(\mathbf{r},\mathbf{r}',i\omega)$ is the non–interacting Green function, which is given by

$$[G_0^{-1}]^{\sigma\sigma'}(\mathbf{r},\mathbf{r}',\omega) = [(\omega+\mu+\nabla^2 - V_{ext}(\mathbf{r}))\delta_{\sigma\sigma'} - \xi\mathbf{l}\cdot\mathbf{s}_{\sigma\sigma'} - g\mu_B\mathbf{B}_{ext}\mathbf{s}_{\sigma\sigma'}]\delta(\mathbf{r}-\mathbf{r}') \tag{45}$$

Since $\mathcal{G}$ is a functional of G_{loc}, it is very useful to view the spectral density functional Γ_{SDF} as a functional of $\mathcal{G}$:

$$\Gamma_{SDF}[\mathcal{G}] = \mathrm{Tr}\ln\mathcal{G} - \mathrm{Tr}[G_0^{-1} - \mathcal{G}^{-1}]\mathcal{G} + \Phi_{SDF}[G_{loc}] \tag{46}$$

where the first two contribution represent the kinetic contribution and the contribution from the external potential and magnetic field. The unknown interaction part of the free energy $\Phi_{SDF}[G_{loc}]$ is the functional of G_{loc}. If the Hartree term is explicitly extracted, this functional can be represented as

$$\Phi_{SDF}[G_{loc}] = E_H[\rho] + \Phi^{xc}_{SDF}[G_{loc}] \tag{47}$$

To facilitate the calculation, the auxiliary Green function $\mathcal{G}^{\sigma\sigma'}(\mathbf{r},\mathbf{r}',i\omega)$ can be represented in terms of generalized energy–dependent one–particle states

$$\mathcal{G}^{\sigma\sigma'}(\mathbf{r},\mathbf{r}',i\omega) = \sum_{\mathbf{k}j}\frac{\psi^{R(\sigma)}_{\mathbf{k}j\omega}(\mathbf{r})\psi^{L(\sigma')}_{\mathbf{k}j\omega}(\mathbf{r}')}{i\omega+\mu-E_{\mathbf{k}j\omega}} \tag{48}$$

which obey the one–particle Dyson equation for the "right" eigenvector $\psi^{R(\sigma)}_{\mathbf{k}j\omega}(\mathbf{r})$

$$\sum_{\sigma'}\{[-\nabla^2 + V_{ext}(\mathbf{r}) + V_H(\mathbf{r})]\delta_{\sigma\sigma'} + g\mu_B\mathbf{B}_{eff}\mathbf{s}_{\sigma\sigma'} + \xi\mathbf{l}\cdot\mathbf{s}_{\sigma\sigma'}\}\psi^{R(\sigma')}_{\mathbf{k}j\omega}(\mathbf{r}) + \tag{49}$$

$$\sum_{\sigma'}\int d\mathbf{r}'\mathcal{M}^{\sigma\sigma'}_{xc}(\mathbf{r},\mathbf{r}',i\omega)\psi^{R(\sigma')}_{\mathbf{k}j\omega}(\mathbf{r}') = E_{\mathbf{k}j\omega}\psi^{R(\sigma)}_{\mathbf{k}j\omega}(\mathbf{r}) \tag{50}$$

and similar equation for the "left" eigenvector $\psi^{L(\sigma)}_{\mathbf{k}j\omega}(\mathbf{r})$ when it appears on the left.

Evaluation of the free energy requires writing down the precise functional form for $\Phi_{SDF}[G_{loc}]$. Unfortunately, it is a problem because the free energy $F = E - TS$, where E is the total energy and S is the entropy, and the evaluation of the entropy requires the evaluation of the energy as a function of temperature and an additional integration over it. However, the total energy formula can be written by utilizing the Galitzky–Migdal expression for the interaction energy[5]. It is given by:

$$E = T\sum_{i\omega}e^{i\omega 0^+}\sum_{\mathbf{k}j}g_{\mathbf{k}j\omega}E_{\mathbf{k}j\omega} - T\sum_{i\omega}\sum_{\sigma\sigma'}\int d\mathbf{r}d\mathbf{r}'\mathcal{M}^{\sigma\sigma'}_{eff}(\mathbf{r},\mathbf{r}',i\omega)\mathcal{G}^{\sigma'\sigma}(\mathbf{r}',\mathbf{r},i\omega) +$$
$$+\int d\mathbf{r}V_{ext}(\mathbf{r})\rho(\mathbf{r}) - \int d\mathbf{r}\mathbf{B}_{ext}(\mathbf{r})\mathbf{m}(\mathbf{r}) + E_H[\rho] + \frac{1}{2}T\sum_{i\omega}\sum_{\sigma\sigma'}\int d\mathbf{r}d\mathbf{r}'\mathcal{M}^{\sigma\sigma'}_{xc}(\mathbf{r},\mathbf{r}',i\omega)\mathcal{G}^{\sigma'\sigma}(\mathbf{r}',\mathbf{r},i\omega) \tag{51}$$

where

$$g_{\mathbf{k}j\omega} = \frac{1}{i\omega + \mu - E_{\mathbf{k}j\omega}} \tag{52}$$

We have cast the notation of spectral density theory in a form similar to DFT. The function $g_{\mathbf{k}j\omega}$ is the Green function in the orthogonal left/right representation which plays a role of a "frequency dependent occupation number".

Both the charge density and non–collinear magnetization can be found from the integral over the $\mathbf{k}$–space:

$$\rho(\mathbf{r}) = T\sum_{i\omega}\sum_{\mathbf{k}j}\sum_{\sigma}g_{\mathbf{k}j\omega}\psi^{L(\sigma)}_{\mathbf{k}j\omega}(\mathbf{r})\psi^{R(\sigma)}_{\mathbf{k}j\omega}(\mathbf{r})e^{i\omega 0^+} \tag{53}$$

$$\mathbf{m}(\mathbf{r}) = g\mu_B T\sum_{i\omega}\sum_{\mathbf{k}j}g_{\mathbf{k}j\omega}\sum_{\sigma\sigma'}\mathbf{s}_{\sigma\sigma'}\psi^{L(\sigma)}_{\mathbf{k}j\omega}(\mathbf{r})\psi^{R(\sigma')}_{\mathbf{k}j\omega}(\mathbf{r})e^{i\omega 0^+} \tag{54}$$

The central procedure which is yet to be determined is the construction of the exchange–correlation part of the self–energy. It is formally a variational derivative of the exchange correlation part of the free energy functional

$$\mathcal{M}^{\sigma\sigma'}_{xc}(\mathbf{r},\mathbf{r}',i\omega) = \frac{\delta\Phi^{xc}_{SDF}[G_{loc}]}{\delta\mathcal{G}^{\sigma'\sigma}(\mathbf{r}',\mathbf{r},i\omega)} = \frac{\delta\Phi^{xc}_{SDF}[G_{loc}]}{\delta G^{\sigma'\sigma}_{loc}(\mathbf{r}',\mathbf{r},i\omega)}\theta_{loc}(\mathbf{r},\mathbf{r}') \tag{55}$$

The spectral density functional theory, where an exact functional of certain local quantities is constructed in the spirit of Ref. 90 uses effective self–energies which are local by construction. This property can be exploited to find good approximations to the interaction energy functional. For example, if it is *a priori* known that the real electronic self–energy is local in a certain portion of the Hilbert space, a good approximation is the corresponding local dynamical mean field theory obtained for example by a restriction or truncation of the full Baym–Kadanoff functional to local quantities in the spirit of Ref. 91.The local DMFT approximates the functional $\Phi_{SDF}[G_{loc}]$ by the sum of all two–particle diagrams evaluated with G_{loc} and the bare Coulomb interaction v_C . In other words, the functional dependence of the interaction part $\Phi_{BK}[G]$ in the Baym–Kadanoff functional for which the diagrammatic rules exist is now restricted by G_{loc} and is used as an approximation to $\Phi_{SDF}[G_{loc}]$, i.e. $\Phi_{SDF}[G_{loc}] = \Phi_{BK}[G_{loc}]$. Obviously that the variational derivative of such restricted functional will generate the self–energy confined in the same area as the local Green function itself.

Remarkably the summation over all local diagrams can be performed exactly via introduction of an auxiliary quantum impurity model subjected to a self–consistency condition[5]. If this impurity is considered as a cluster C, the cellular DMFT (C–DMFT) can be used which breaks the translational invariance of the lattice to obtain accurate estimates of the self energies.

Various methods such as LDA+U[2], LDA+DMFT[94] and local GW[92,95] which appeared recently for realistic calculations of properties of strongly correlated materials can be naturally understood within spectral density functional theory. Let us, for example, explore the idea of expressing the energy as the density functional. Local density approximation prompts us that a large portion of the exchange–correlation part $\Phi_{xc}[\rho]$ can be found easily. Indeed, the charge density is known to be accurately obtained by the LDA. Why not think of LDA as the most primitive impurity solver, which generates manifestly local self–energy with localization radius collapsed to a single $\mathbf{r}$ point? It is tempting to represent $\Phi_{SDF}[G_{loc}] = E_H[\rho] + E_{xc}^{LDA}[\rho] + \tilde{\Phi}[G_{loc}] - \Phi_{DC}[G_{loc}]$, where the new functional $\tilde{\Phi}_{SDF}[G_{loc}]$ needs in fact to take care of those electrons which are strongly correlated and heavy, thus badly described by LDA. Conceptually, that means that the solution of the cluster impurity model for the light electrons is approximated by LDA and does not need a frequency resolution for their self–energies.

Such introduced LDA+DMFT approximation considers both the density and the local Green function as the parameters of the spectral density functional . A further approximation is made to accelerate the solution of a single–site impurity model: the functional dependence comes from the subblock of the correlated electrons only. If localized orbital representation $\{\chi_\alpha\}$ is utilized, a subspace of the heavy electrons $\{\chi_a\}$ can be identified. Thus, the approximation can be written as $\tilde{\Phi}_{SDF}[G_{loc,ab}(i\omega)]$, where $G_{loc,ab}(i\omega)$ is the heavy block of the local Green function.

Unfortunately, the LDA has no diagrammatic representation, and it is difficult to separate the contributions from the light and heavy electrons. The $E_{xc}^{LDA}[\rho]$ is a non–linear functional and it already includes the contribution to the energy from all orbitals in some average form. Therefore we need to take care of a non–trivial double counting, encoded in the functional $\Phi_{DC}[G_{loc}]$. The precise form of the double counting is related to the approximation imposed for $\tilde{\Phi}[G_{loc}]$ and can be borrowed from the LDA+U method[2]. Note that both LDA+U and LDA+DMFT methods require separations of the electrons onto light and heavy which makes them basis–set dependent.

Iron and nickel were studied in Refs. 96,97. The values $U = 2.3$ (3.0) eV for Fe (Ni) and the same value of the interatomic exchange, $J = 0.9$ eV for both Fe and Ni were used, as came out from the constrained LDA calculations[89,98,99]. These parameters are consistent with those of many earlier studies and resulted in a good description of the physical properties of Fe and Ni. In Ref. 97 the general form of the double counting correction $V_\sigma^{DC} = \frac{1}{2} Tr_\sigma \mathcal{M}_\sigma(0)$ was taken. Notice that because of the different self energies in the e_g and t_{2g} blocks the DMFT Fermi surface does not coincide with the LDA Fermi surface.

The impurity model was solved by QMC in Ref. 97 and by the FLEX scheme in Ref. 100. It is clear that nickel is more itinerant than iron (the spin–spin autocorrelation decays faster), which has longer lived spin fluctuations. On the other hand, the one–particle density of states of iron resembles very much the LSDA density of states while the DOS of nickel below T_c, has additional features which are not present in the LSDA spectra[101,102,103]: the presence of a famous 6 eV satellite, the 30% narrowing of the occupied part of d-band and the 50% decrease of exchange spittoons compared to the LDA results. Note that the satellite in Ni has substantially more spin-up contributions in agreement with photoemission spectra[103]. The exchange splitting of the d–band depends very weakly on temperature from $T = 0.6T_C$ to $T = 0.9T_C$. Correlation effects in Fe are less pronounced than in Ni, due to its large spin splitting and the characteristic bcc structural dip in the density of states for the spin–down states near the Fermi level, which reduces the density of states for particle hole excitations.

The uniform spin susceptibility in the paramagnetic state, $\chi_{q=0} = dM/dH$, was extracted from the QMC simulations by measuring the induced magnetic moment in a small external magnetic field. It includes the polarization of the impurity Weiss field by the external field[5]. The dynamical mean field results account for the Curie–Weiss law which is observed experimentally in Fe and Ni. As the temperature increases above T_c, the atomic character of the system is partially restored resulting in an atomic like susceptibility with an effective moment:

$$\chi_{q=0} = \frac{\mu_{eff}^2}{3(T - T_C)}. \tag{56}$$

The temperature dependence of the ordered magnetic moment below the Curie temperature and the inverse of the uniform susceptibility above the Curie point are plotted in Fig. 8 together with the corresponding experimental data for iron and nickel[104]. The LDA+DMFT calculation describes the magnetization curve and the slope of the high–temperature Curie–Weiss susceptibility remarkably well. The calculated values of high–temperature magnetic moments extracted from the uniform spin susceptibility are $\mu_{eff} = 3.09$ (1.50)μ_B for Fe (Ni), in good agreement with the experimental data $\mu_{eff} = 3.13$ (1.62)μ_B for Fe (Ni)[104].

The Curie temperatures of Fe and Ni were estimated from the disappearance of spin polarization in the self–consistent solution of the DMFT problem and from the Curie–Weiss law in Eq.(56). The estimates for $T_C = 1900$ (700) K are in reasonable agreement with experimental values of 1043 (631) K for Fe (Ni) respectively[104], considering the single–site nature of the DMFT approach, which is not able to capture the reduction of T_C due to long–wavelength spin waves. These effects are governed by the spin–wave stiffness. Since the ratio of the spin–wave stiffness D to T_C, $T_C/a^2 D$, is nearly a factor of 3 larger for Fe than for Ni[104] (a is the lattice constant), we expect the T_C in DMFT to

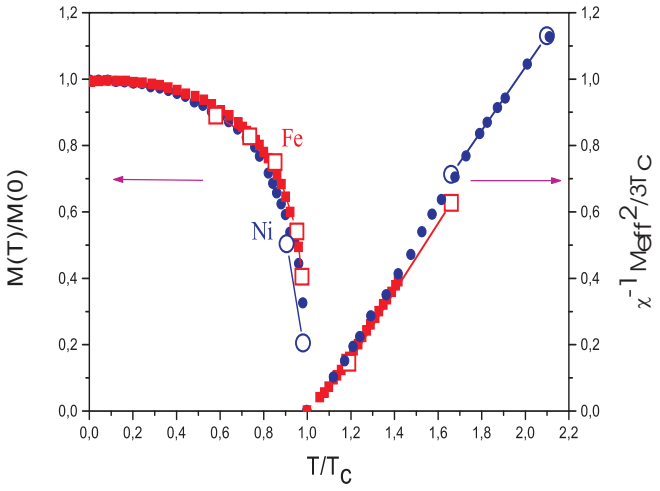

FIG. 8: Temperature dependence of ordered moment and the inverse ferromagnetic susceptibility for Fe (open square) and Ni (open circle) compared with experimental results for Fe (square) and Ni (circle) (from Ref. **?**). The calculated moments were normalized to the LDA ground state magnetization (2.2 μ_B for Fe and 0.6 μ_B for Ni).

be much higher than the observed Curie temperature in Fe than in Ni. Quantitative calculations demonstrating the sizeable reduction of T_C due to spin waves in Fe in the framework of a Heisenberg model were performed in Ref. 41. This physics whereby the long wavelength fluctuations renormalize the critical temperature would be reintroduced in the DMFT by the use E–DMFT. Alternatively, the reduction of the critical temperature due to spatial fluctuations can be investigated with cluster DMFT methods.

Within the dynamical mean field theory one can also compute the local spin susceptibility defined by

$$\chi_{loc} = \frac{g^2}{3} \int_0^\beta d\tau \, \langle \mathbf{S}(\tau) \, \mathbf{S}(0) \rangle \tag{57}$$

where $\mathbf{S} = \frac{1}{2} \sum_{m,\sigma,\sigma'} c^\dagger_{m\sigma} \boldsymbol{\sigma}_{\sigma\sigma'} c_{m\sigma'}$ is single-site spin operator. It differs from the $q = 0$ susceptibility by the absence of spin polarization in the Weiss field of the impurity model. Eq.(57) cannot be probed directly in experiments but it is easily computed within the DMFT–QMC. Its behavior as a function of temperature gives a very intuitive picture of the degree of correlations in the system. In a weakly correlated regime we expect Eq.(57) to be nearly temperature independent, while in a strongly correlated regime we expect a leading Curie–Weiss behavior at high temperatures $\chi_{local} = \mu^2_{loc}/(3T + const.)$ where μ_{loc} is an effective local magnetic moment. In the Heisenberg model with spin S, $\mu^2_{loc} = S(S+1)g^2$ and for the well–defined local magnetic moments (e.g., for rare–earth magnets) this quantity should be temperature independent. For the itinerant electron magnets, μ_{loc} is temperature dependent due to a variety of competing many–body effects such as Kondo screening, the induction of local magnetic moment by temperature[8] and thermal fluctuations which disorder the moments[105]. All these effects are included in the DMFT calculations.

The comparison of the values of the local and the $q = 0$ susceptibility gives a crude measure of the degree of short–range order which is present above T_C. As expected, the moments extracted from the local susceptibility Eq.(57) are a bit smaller (2.8 μ_B for iron and 1.3 μ_B for nickel) than those extracted from the uniform magnetic susceptibility. This reflects the small degree of the short–range correlations which remain well above T_C[106]. The high–temperature LDA+DMFT clearly shows the presence of a local moment above T_C. This moment is correlated with the presence of high–energy features (of the order of the Coulomb energies) in the photoemission. This is also true below T_C, where the spin dependence of the spectra is more pronounced for the satellite region in Nickel than for that of the quasiparticle bands near the Fermi level. This can explain the apparent discrepancies between different experimental determinations of the high–temperature magnetic splittings[107,108,109,110] as being the results of probing different energy regions. The resonant photoemission experiments[109] reflect the presence of local–moment polarization in the high–energy spectrum above the Curie temperature in Nickel, while the low–energy angle resolved photoemission investigations[110] results in non–magnetic bands near the Fermi level. This is exactly the DMFT view on the electronic structure of transition metals above T_C. Fluctuating moments and atomic–like configurations are large at short times, which results in correlation effects in the high–energy spectra such as spin–multiplet splittings.

The moment is reduced at longer time scales, corresponding to a more band–like, less correlated electronic structure near the Fermi level.

NiO and MnO represent two classical Mott–Hubbard systems. Both materials are insulators with the energy gap of a few eV regardless whether they are antiferro– or paramagnetic. The spin dependent LSDA theory strongly underestimates the energy gap in the ordered phase. This can be corrected by the use of the LDA+U method. Both theories however fail completely to describe the local moment regime reflecting a general drawback of band theory to reproduce atomic limit. Therefore the real challenge is to describe the paramagnetic insulating state where the self–energy effects are crucial both for the electronic structure and for recovering the correct phonon dispersions in these materials. The DMFT calculations have been performed[111] by taking into account correlations among d–electrons. In the regime of large U adequate for both for NiO and MnO in the paramagnetic phase the correlations were treated within the well–known Hubbard I approximation.

The calculated densities of states using the LDA+DMFT method for the paramagnetic state of NiO and MnO[111] have revealed the presence of both lower and upper Hubbard subbands. These were found in agreement with the LDA+U calculations of Anisimov[2] which have been performed for the ordered states of these oxides. Clearly, spin integrated spectral functions do not show an appreciable dependence with temperature and look similar below and above phase transition point.

The progress in the electronic structure calculation with DMFT allowed to apply the method to more complicated systems such as plutonium[112,113]. The temperature dependence of atomic volume in Pu is anomalous[114,115]. It shows an enormous volume expansion between α and δ phases which is about 25%. Within the δ phase, the metal shows negative thermal expansion. Transition between δ and higher–temperature ε phase occurs with a 5% volume collapse. Also, Pu shows anomalous resistivity behavior[116] characteristic for the heavy fermion systems, but neither of its phases is magnetic. The susceptibility is small and relatively temperature independent. The photoemission[117] shows a strong narrow Kondo–like peak at the Fermi level consistent with large values of the linear specific heat coefficient.

Density functional based LDA and GGA calculations describe the properties of Pu incorrectly. They predict magnetic ordering[118]. They underestimate[119] equilibrium volume of the δ and ε phase by as much as 30%, the largest discrepancy known in LDA, which usually predicts the volume of solids within a few % accuracy even for such correlated systems as high temperature superconductors.

To address these questions several approaches have been developed. The LDA+U method was applied to δ Pu[120]. It is able to produce the correct volume of the δ phase for values of the parameter $U\tilde{}4$ eV consistent with atomic spectral data and constrained density functional calculations. Similar calculation has been performed by a so–called orbitally ordered density functional method[121]. However, both methods predict Pu to be magnetic, which is not observed experimentally. The LDA+U method is unable to predict the correct excitation spectrum. Also, to recover the α phase within LDA+U the parameter U has to be set to zero which is inconsistent with its transport properties and with microscopic calculations of this parameter. Another approach proposed[122] in the past is the constrained LDA approach in which some of the 5f electrons, are treated as core, while the remaining are allowed to participate in band formation. Results of the self–interaction–corrected LDA calculations have been reported[123], as well as qualitative discussion of the bonding nature across the actinides series has been given[124].

Dynamical mean–field calculations have been recently applied with success to this material. They were performed in paramagnetic state and do not impose magnetic ordering. DMFT was able to predict the appearance of a strong quasiparticle peak near the Fermi level which exists in the both phases. Also, the lower and upper Hubbard bands were clearly distinguished. The width of the quasiparticle peak in the α phase is found to be larger by 30 per cent compared to the width in the δ phase. This indicates that the low–temperature phase is more metallic, i.e. it has larger spectral weight in the quasiparticle peak and smaller weight in the Hubbard bands. Recent advances have allowed the experimental determination of these spectra, and these calculations were consistent with these measurements[117].

VIII. CONCLUSION

In conclusion, electronic structure methods have been applied with success to study magnetic properties of solids. Many good results have been obtained for weakly correlated itinerant systems. New algorithms for inclusion of many–body effects are beginning to attack magnetic phenomena in strongly correlated materials. These successes have generated a new synergy between the electronic structure and many–body communities, which are jointly developing new and powerful electronic structure tools for virtual material exploration.

The work on magnetic anisotropy was supported by the Office of Naval Research grant No. 4-2650.

---

[1] *Theory of the Inhomogeneous Electron Gas* (Eds. S. Lundqvist, S. H. March). Plenum, New York, 1983.

[2] For a review, see, e.g., *Strong Correlations in electronic structure calculations*(Ed. V. I. Anisimov). Gordon and Breach Science Publishers, Amsterdam, 2000.

[3] Sandratskii, L. M.: Energy band structure calculations for crystals with spiral magnetic structure. Phys. Stat. Sol. (b) **135** (1986) 167-180.

[4] Liechtenstein, A. I.; Katsnelson, M. I.; Antropov, V. P.; Gubanov, V. A.: Local spin density functional approach to the theory of exchange interactions in ferromagnetic metals and alloys. J. Magn. Magn. Mater. **67** (1987) 65-74 .

[5] For a review, see, e.g., Georges, A.; Kotliar, G.; Krauth, W.; Rozenberg, M.: Dynamical mean-field theory of strongly correlated fermion systems and the limit of infifnite dimensions. Rev. Mod. Phys. **68** (1996) 13-125.

[6] For a review, see, e.g., Antropov, V.P.; Harmon, B.N.; Smirnov, A.N.: Aspects of spin dynamics and magnetic interactions. J. Magn. Magn. Mater. **200** (1999) 148-166.

[7] For a review, see, e.g., Sandratskii, L. M.: Noncollinear magnetism in itinerant-electron systems: theory and applications. Adv. Phys. **47** (1998) 91-160.

[8] For a review, see, e.g., Moriya, T.: Spin Fluctuations in Itinerant Electron Magnetism. Springer, Berlin, 1985.

[9] For a review, see, e.g., Kübler, J.: Theory of Itinerant Electron Magnetism. Oxford University Press, 2000.

[10] Nordstrom, L.; Singh, D. J.: Noncollinear Intra-atomic Magnetism. Phys. Rev. Lett. **76** (1996) 4420-4423 .

[11] Andersen, O. K.: Linear methods in band theory. Phys. Rev. B **12** (1975) 3060-3083.

[12] Koelling, D. D.; Harmon, B. N.: A technique for relativistic spin-polarised calculations. J. Phys. C: Solid State Phys. **10** (1977) 3107-3114.

[13] van Vleck, J. H.: On the anisotropy of cubic ferromagnetic crystals. Phys. Rev. **52** (1937) 1178-1198.

[14] Brooks, V.: Ferromagnetic Anisotropy and the Itinerant Electron Model. Phys. Rev. **58** (1940) 909-918.

[15] G. C. Fletcher, Proc. R. Soc. London **67A**, 505 (1954).

[16] J. C. Sloncewskij, J. Phys. Soc. Jpn. **17**, Suppl. B (1962).

[17] Asdente, M.; Delitala, M.: Magnetocrystalline energy, electronic charge distribution, and Fermi surface of iron from a tight-binding calculation. Phys. Rev. **163** (1967) 497-503.

[18] Eckardt, H.; Fritsche, L.; Noffke, J.: A relativistic treatment of interacting spin-aligned electron systems: application to ferromagnetic iron, nickel and palladium metal. J. Phys. F **17** (1987) 943-966.

[19] Halilov, S. V.; Perlov, A. Ya.; Oppeneer, P. M.; Yaresko, A. N.; Antonov, V. N.: Magnetocrystalline anisotropy energy in cubic Fe, Co, and Ni: Applicability of local-spin-density theory reexaminedPhys. Phys. Rev. B **57** (1998) 9557-9560.

[20] Jansen, H. J. F.: Origin of orbital momentum and magnetic anisotropy in transition metals. J. Appl. Phys. **67** (1990) 4555-4557.

[21] Trygg, J.; Johansson, B.; Eriksson, O.; Willis, J. M.: Total energy calculation of the magnetocrystalline anisotropy energy in the ferromagnetic 3d metals. Phys. Rev. Lett. **75** (1995) 2871-2874.

[22] Daalderop, G. H. O.; Kelly, P. J.; Schuurmans, M. F. H.: First-principles calculation of the magnetocrystalline anisotropy energy of iron, cobalt, and nickel. Phys. Rev. B **41** (1990) 11919-11937.

[23] Wang, D.; Wu, R.; Freeman, A. J.: State-tracking first-principles determination of magnetocrystalline anisotropy. Phys. Rev. Lett. **70** (1993) 869-872.

[24] Beiden, S. V.; Temmerman, W. M.; Szotek, Z.; Gehring, G. A.; Stocks, G. M.; Wang, Y.; Nicholson, D. M. C; Shelton, W. A.; Ebert, H.: Real-space approach to the calculation of magnetocrystalline anisotropy in metals. Phys. Rev. B **57** (1998) 14247-14253.

[25] Pajda, M.; Kudrnovsky, J.; Turek, I.; Drchal, V.; Bruno, P.: cond-mat/0007441.

[26] Katsnelson, M. I.; Lichtenstein, A. I.: LDA++ approach to the electronic structure of magnets: correlation effects in iron. J. Phys. Cond. Matt. **11** (1999) 1037-1048.

[27] Schwarz, K.: CrO_2 predicted as a half-metallic ferromagnet. J. Phys. F: Met. Phys. **16** (1986) L211-L215.

[28] Lewis, S. P.; Allen, P. B.; Sazaki, T.: Band structure and transport properties of CrO_2. Phys. Rev. B **55** (1997) 10253-10260.

[29] Korotin, M. A.; Anisimov, V. I.; Khomskii, D. I.; Sawatzky, G. A.: CrO_2: A Self-Doped Double Exchange Ferromagnet. Phys. Rev. Lett. **80** (1997) 4305-4308.

[30] Mazin, I. I.; Singh, D. J.: Transport, optical, and electronic properties of the half-metal CrO_2. Phys. Rev. B **59** (1999) 411-418.

[31] Craco, L.; Laad, M. S.; Muller-Hartmann, E.: Orbital Kondo Effect in CrO_2: A Combined Local-Spin-Density-Approximation Dynamical-Mean-Field-Theory Study. Phys. Rev. Lett. **90** (2003) 237203-237206.

[32] Cloud, W. H.; Schreider, D. S.; Babcock, K. R.: X-ray and magnetic studies of CrO_2 single crystals. J. Appl. Phys. **33** (1962) 1193-1194.

[33] Spinu, L.; Srikanth, H.; Gupta, A.; Li, X. W.; Gang Xiao: Probing magnetic anisotropy effects in epitaxial CrO_2 thin films. Phys. Rev. B **62** (2000) 8931-8934.

[34] Yang, F. Y.; Chien, C. L.; Ferrari, E. F.; Li, X. W.; Gang Xiao; Gupta, A.: Uniaxial anisotropy and switching behavior in epitaxial CrO_2 films. Appl. Phys. Lett. **77** (2000) 286-288.

[35] Li, X. W.; Gupta, A.; Giang Xiao: Influence of strain on the magnetic properties of epitaxial (100) chromium dioxide

(CrO_2) films. Appl. Phys. Lett. **75** (1999) 713-715.
[36] Halilov, S. V.; Perlov, A. Y.; Oppeneer, P. M.; Eschrig, H.: Magnon spectrum and related finite-temperature magnetic properties: A first-principle approach. Europhys. Lett. **39** (1997) 91-96.
[37] Halilov, S. V.; Eschrig, H.; Perlov, A. Y.; Oppeneer, P. M.: Adiabatic spin dynamics from spin-density-functional theory: Application to Fe, Co, and Ni. Phys. Rev. B **58** (1998) 293-302.
[38] Lynn, J. W.: Temperature dependence of the magnetic excitations in iron. Phys. Rev. B **11** (1975) 2624-2637; Loong, C.-K.; Carpenter, J. M.; Lynn, J. W.; Robinson, R. A.; Mook, H. A.: Neutron scattering study of the magnetic excitations in ferromagnetic iron at high energy transfers. J. Appl. Phys. **55** (1984) 1895-1897.
[39] Rosengaard, N. M.; Johansson, B.: Finite-temperature study of itinerant ferromagnetism in Fe, Co, and Ni. Phys. Rev. B **55**(1997) 14975-14986.
[40] Antropov, V. P.; Katsnelson, M. I.; van Schilfgaarde, M.; Harmon, B. N.: *Ab Initio* Spin Dynamics in Magnets. Phys. Rev. Lett. **75** (1995) 729-732.
[41] Pajda, M.; Kudrnovsky, J.; Turek, I.; Drchal, V.; Bruno, P.: Ab initio calculations of exchange interactions, spin-wave stiffness constants, and Curie temperatures of Fe, Co, and Ni. Phys. Rev. B **64** (2001) 174402-174410.
[42] Sandratskii, L. M.; Bruno, P.: Electronic structure, exchange interactions, and Curie temperature in diluted III-V magnetic semiconductors: (GaCr)As, (GaMn)As, (GaFe)As. Phys. Rev. B **67** (2003) 214402-214412; Sandratskii, L. M.; Bruno, P.; Kudrnovsky, J.: On-site Coulomb interaction and the magnetism of (GaMn)N and (GaMn)As. Phys. Rev. B **69** (2004) 195203-195209.
[43] Pederson, M. R.; Bernstein, N.; Kortus, J.: Fourth-order magnetic anisotropy and tunnel splittings in Mn12 from spin-orbit-vibron interactions. Phys. Rev. Lett. **89** (2002) 097202-097205; Boukhvalov, D. W.; Lichtenstein, A. I.; Dobrovitski, V. V.; Katsnelson, M. I.; Harmon, B. N.; Mazurenko, V. V.; Anisimov, V. I.: Effect of local Coulomb interactions on the electronic structure and exchange interactions in Mn12 magnetic molecules. Phys. Rev. B **65** (2002) 184435-184440.
[44] Solovyev, I. V.; Terakura, K.: Spin canting in three-dimensional perovskite manganites. Phys. Rev. B **63** (2001) 174425-174441.
[45] Umetsu, R. Y.; Fukamichi, K.; Fujinaga, Y.; Sakuma, A.: Magnetovolume effects and spin fluctuations in $Mn_{3+x}Rh_{1-x}$ alloys. J. Phys: Condens Matter **15** (2003) 4589-4604.
[46] Skomski, R.; Kashyap, A.; Sellmyer, D. J.: Finite-temperature anisotropy of PtCo magnets. IEEE Trans. Magnet. **39** (2003) 2917-2919.
[47] Callaway J.; Wang, C. S.; Laurent, D. G.: Magnetic susceptibility and spin waves in ferromagnetic metals. Phys. Rev. B **24** (1981) 6491-6496.
[48] Cooke, J. F.; Lynn, J. W. ; Davis, H. L.: Calculations of the dynamic susceptibility of nickel and iron. Phys. Rev. B **21** (1980) 4118-4131.
[49] Savrasov, S. Y.: Linear Response Calculations of Spin Fluctuations. Phys. Rev. Lett. **81** (1998) 2570-2573.
[50] Runge, E.; Gross, E. K. U.: Density-Functional Theory for Time-Dependent Systems. Phys. Rev. Lett. **52** (1984) 997-1000; Gross, E. K. U.; Kohn, W.: Local density-functional theory of frequency-dependent linear response. Phys. Rev. Lett. **55** (1984) 2850-2852.
[51] Bruno, P.: Exchange interaction parameters and adiabatic spin-wave spectra of ferromagnets: A "Renormalized Magnetic Force theorem". Phys. Rev. Lett. **90** (2003) 087205-087208.
[52] Antropov, V. P.: The exchange coupling and spin waves in metallic magnets: removal of the long-wave approximation. J. Magn. Magn. Mater. **262** (2003) L192-L197.
[53] Cooke, J. F.: Neutron scattering from itinerant-electron ferromagnets. Phys. Rev. B **7** (1973) 1108-1116.
[54] Callaway, J.; Wang, C. S.: Transverse magnetic susceptebility in the local exchange approximation. J. Phys. F: Met. Phys. **5** (1975) 2119-2128; Callaway, J.; Chatterjee, A. K.: Dynamic longitudinal spin susceptebility of Bloch electrons. J. Phys. F: Met. Phys. **8** (1978) 2569-2577.
[55] Callaway, J.; Chatterjee, A. K.; Singhal, S. P.; Ziegler, A.: Magnetic susceptibility of ferromagnetic metals: Application to nickel. Phys. Rev. B **28** (1983) 3818-3830.
[56] Stenzel, E.; Winter, H.: The wave vector dependent spin susceptibilities of Pd and V and their contributions to the low temperature specific heat. J. Phys. F: Met. Phys. **16** (1986) 1789-1809.
[57] Savrasov, S. Y.: Linear response calculations of lattice dynamics using muffin-tin basis sets Phys. Rev. Lett. **69** (1992) 2819-2822; Savrasov, S. Y.: Linear-response theory and lattice dynamics: A muffin-tin-orbital approach. Phys. Rev. B **54** (1996) 16470-16486.
[58] Dobson, J.: Harmonic-Potential Theorem: Implications for Approximate Many-Body Theories. Phys. Rev. Lett. **73** (1994) 2244-2247 ; Vignale, G.; Kohn, W.: Current-Dependent Exchange-Correlation Potential for Dynamical Linear Response Theory. Phys. Rev. Lett. **77** (1996) 2037-2040.
[59] Oudovenko, V.; Savrasov, S. Y.: Linear-response calculation of dynamical spin susceptibility in doped $CaCuO_2$. Phys. Rev. B **63** (2001) 132401-132404.
[60] Perdew, J. P.; Burke, K.; Ernzerhof, M.: Generalized Gradient Approximation Made Simple. Phys. Rev. Lett. **77** (1996) 3865-3868.
[61] Vosko, S. H.; Perdew, J. P.: Theory of spin susceptibility of an inhomogenious electron gas via the density functional formalism. Can. J. Phys. **53** (1975) 1385-1397.
[62] Gonze, X.; Allan, D. C.; Teter, M. P.: Dielectric tensor, effective charges, and phonons in alpha -quartz by variational density-functional perturbation theory. Phys. Rev. Lett. **68** (1992) 3603-3606.
[63] See, *e.g.*: Gonze, X.: Adiabatic density-functional perturbation theory. Phys. Rev. A **52** (1995) 1096-1114.
[64] Liu, K. L.; Vosko, S. H.: A time-dependent spin density functional theory for the dynamical spin susceptibility. Can. J.

Phys. **67** (1989) 1015-1021.
[65] Mook, H. A.; Paul, D. McK.: Neutron-scattering measurement of the spin-wave spectra for nickel. Phys. Rev. Lett. **54** (1985) 227–229.
[66] See, *e.g.*: Fawcett, E.: Spin-density-wave antiferromagnetism in chromium. Rev. Mod. Phys. **60** (1988) 209-283.
[67] Staunton, J. B.; Poulter, J.; Ginatempo, B.; Bruno, E.; Johnson, D. D.: Incommensurate and commensurate antiferromagnetic spin fluctuations in Cr and Cr alloys from *Ab Initio* dynamical spin susceptibility calculations. Phys. Rev. Lett. **82** (1999) 3340-3343.
[68] Hubbard, J.: The magnetism of iron. Phys. Rev. B **19** (1979) 2626-2636; Hubbard, J.: Magnetism of iron. II. Phys. Rev. B **20** (1979) 4584-4595; Hubbard, J.: Magnetism of nickel. Phys. Rev. B**23** (1981) 5974-5977.
[69] Stratonovich, R. L.: On a method of calculating quantum distribution functions. Sov. Phys. Dokl. **2** (1958) 416-419.
[70] Wang, S. Q.; Evenson, W. E.; Schrieffer, J. R.: Theory of itinerant ferromagnets exhibiting localized-moment behavior above the Curie point. Phys. Rev. Lett. **23** (1969) 92-95.
[71] Evenson, W. E.; Wang, S. Q.; Schrieffer, J. R.: Theory of itinerant ferromagnets with localized-moment characteristics: two-center coupling in the functional-integral scheme. Phys. Rev. B **2** (1970) 2604-2606.
[72] Cyrot, M.: Phase transition in Hubbard model. Phys. Rev. Lett. **25** (1970) 871-874.
[73] Al-Attar, H.; Kakehashi, Y.: Magnetic phase diagram of Fe and Ni from crystals to amorphous structures. J. Appl. Phys. **86** (1999) 3265-3273.
[74] Kakehashi, Y.: Monte Carlo approach to the dynamical coherent-potential approximation in metallic magnetism. Phys. Rev. B **45** (1992) 7196-7204; Kakehashi, Y.: Dynamical coherent-potential approximation to the magnetism in a correlated electron system. Phys. Rev. B **65** (2002) 184420-184435; Kakehashi, Y.; Akbar, S.; Kimura, N.: Molecular-dynamics approach to itinerant magnetism with complex magnetic structures. Phys. Rev. B **57** (1998) 8354-8369.
[75] Gyorffy, B. L.; Stocks, G. M.: Electrons in Disordered Metals and at Metallic Surfaces, p. 89. Plenum, New York, NY, USA, 1979.
[76] Faulkner, J. S.: The modern theory of alloys. Prog. Mater. Sci. **27** (1982) 1-187.
[77] Gyorffy, B. L.; Pindor, A. J.; Staunton, J.; Stocks, G. M.; Winter, H.: A first-principle theory of ferromagnetic phase transitions in metals. J. Phys. F: Met. Phys. **15** (1985) 1337-1386.
[78] Staunton, J.; Gyorffy, B. L.; Pindor, A. J.; Stocks, G. M.; Winter, H.: Electronic structure of metallic ferromagnets above the Curie temperature. J. Phys. F: Met. Phys. **15** (1985) 1387-1404.
[79] Capellmann, H.: Ferromagnetism and strong correlations in metals. J. Phys. F: Met. Phys. **4** (1974) 1466-1476.
[80] Korenman, V.; Murray, J. L.; Prange, R. E.: Local-band theory of itinerant ferromagnetism. I. Fermi-liquid theory. Phys. Rev. B **16** (1977) 4032-4047; Korenman, V.; Murray, J. L.; Prange, R. E.: Local-band theory of itinerant ferromagnetism. II. Spin waves. Phys. Rev. B **16** (1977) 4048-4057; Korenman, V.; Murray, J. L.; Prange, R. E.: Local-band theory of itinerant ferromagnetism. III. Nonlinear Landau-Lifshitz equations. Phys. Rev. B **16** (1977) 4058-4062.
[81] Prange, R. E.; Korenman, V.: Local-band theory of itinerant ferromagnetism. V. Statistical mechanics of spin waves. Phys. Rev. B **19** (1979) 4698-4702; Prange, R. E.; Korenman, V.: Local-band theory of itinerant ferromagnetism. IV. Equivalent Heisenberg model. Phys. Rev. B **19** (1979) 4691-4697.
[82] Belitz, D.; Kirkpatrick, T. R.: Fluctuation-driven quantum phase transitions in clean itinerant ferromagnets. Phys. Rev. Lett. **89** (2002) 247202-247205.
[83] Liebsch, A.: Ni d-band self-energy beyond the low-density limit. Phys. Rev. B **23** (1981) 5203-5212.
[84] Manghi, F.; Bellini, V.; Arcangelli, C.: On-site correlation in valence and core states of ferromagnetic nickel. Phys. Rev. B **56** (1997) 7149-7161.
[85] Manghi, F.; Bellini, V.; Osterwalder, J.; Kreutz, T. J.; Arcangeli, C.: Correlation effects in the low-energy region of nickel photoemission spectra. Phys. Rev. B **59** (1999) R10409-R10412.
[86] Nolting, W.; Rex, S.; Jaya, S. M.: Magnetism and electronic structure of a local moment ferromagnet. J. Phys.: Condens. Matter **9** (1987) 1301-1330.
[87] Steiner, M. M.; Albers, R. C.; Sham, L. J.: Quasiparticle properties of Fe, Co, and Ni. Phys. Rev. B **45** (1992) 13272-13284.
[88] Anisimov, V. I.; Poteryaev, A. I.; Korotin, M. A.; Anokhin, A. O.; Kotliar, G.: First-principles calculations of the electronic structure and spectra of strongly correlated systems: dynamical mean-field theory J. Phys.: Condens. Matter **9** (1997) 7359-7368.
[89] Lichtenstein, A. I.; Katsnelson, M. I.: *Ab initio* calculations of quasiparticle band structure in correlated systems: LDA++ approach. Phys. Rev. B **57** (1998) 6884-6895.
[90] Chitra, R.; Kotliar, G.: Dynamical mean-field theory and electronic structure calculations. Phys. Rev. B **62** (2000) 12715-12723.
[91] Chitra, R.; Kotliar, G.: Effective-action approach to strongly correlated fermion systems. Phys. Rev. B **63** (2001) 115110-115118.
[92] Kotliar, G.; Savrasov, S. Y.: Dynamical mean field theory, model hamiltonians and first principles electronic structure calculations. In *New Theoretical approaches to strongly correlated systems* (Ed. A. M. Tsvelik), p. 259. Kluwer Academic Publishers, the Netherlands, 2001; cond–mat/020824.
[93] Savrasov, S. Y.; Kotliar, G.: Spectral density functionals for electronic structure calculations. Phys. Rev. B **69** (2004) 245101-245124.
[94] For a review, see, e.g., Held, H.; Nekrasov, I. A.; Keller, G.; Eyert, V.; Blümer, N.; McMahan, A. K.; Scalettar, R. T.; Pruschke, Th.; Anisimov, V. I.; Vollhardt, D.: The LDA+DMFT Approach to Materials with Strong Electronic Correlations. In *Psi–k Network Newsletter*, June 2003.
[95] Zein, N. E.; Antropov, V. P.: Self-consistent green function approach for calculation of electronic structure in transition

metals. Phys. Rev. Lett. **89** (2002) 126402-126405.
[96] Katsnelson, M. I.; Lichtenstein, A. I.: First-principles calculations of magnetic interactions in correlated systems. Phys. Rev. B **61** (2000) 8906-8912.
[97] Lichtenstein, A. I.; Katsnelson, M. I.; Kotliar, G.: Finite-temperature magnetism of transition metals: An *ab initio* Dynamical mean-field theory. Phys. Rev. Lett. **87** (2001) 067205-067208.
[98] Bandyopadhyay, M. T.; Sarma, D. D.: Calculation of Coulomb interaction strengths for 3d transition metals and actinides. Phys. Rev. B **39** (1989) 3517-3521.
[99] Lichtenstein, A. I.; Katsnelson, M. I.: Dynamical mean field band structure: LDA++ aproach. Bull. Am. Phys. **42** (1997) 573.
[100] M. I. Katsnelson and A. I. Lichtenstein,: Electronic structure and magnetic properties of correlated metals: A local self-consistent perturbation scheme. Eur. Phys. J. B **30** (2002) 9-15.
[101] Iwan, M.; Himpsel, F. J.; Eastman, D. E.: Two-Electron Resonance at the 3p Threshold of Cu and Ni. Phys. Rev. Lett. **43** (1979) 1829-1832.
[102] Eberhardt, W.; Plummer, E. W.: Angle-resolved photoemission determination of the band structure and multielectron excitations in Ni. Phys. Rev. B **21** (1980) 3245–3255.
[103] Altmann, K. N.; Petrovykh, D. Y.; Mankey, G. J.; Shannon, N.; Gilman, N.; Hochstrasser, M.; Willis, R. F.; Himpsel, F. J.: Enhanced spin polarization of conduction electrons in Ni explained by comparison with Cu. Phys. Rev. B **61** (2000) 15661-15666.
[104] Ferromagnetic Materials, (Ed. E. P. Wolfarth) vol 1. North–Holland, Amsterdam, 1986.
[105] Irkhin, V. Y.; Katsnelson, M. I.: Half-metallic ferromagnets. Physics - Uspekhi **37** (1994) 659-676.
[106] H. A. Mook and J. W. Lynn,: Measurements of the magnetic excitations above T_c in iron and nickel (invited). J. Appl. Phys. **57** (1985) 3006-3011.
[107] Kisker, E.; Schröder, K.; Campagna, M.; Gudat, W.: Temperature dependence of the exchange splitting of Fe by spin-resolved photoemission spectroscopy with synchrotron radiation. Phys. Rev. Lett. **52** (1984) 2285–2288.
[108] Kakizaki, A.; Fujii, J.; Shimada, K.; Kamata, A.; Ono, K.; Park, K.; Kinoshita, T.; Ishii, T.; Fukutani, H.: Fluctuating local magnetic moments in ferromagnetic Ni observed by the spin-resolved resonant photoemission. Phys. Rev. Lett. **72** (1994) 2781-2784.
[109] Sinkovic, B.; Tjeng, L. H.; Brookes, N. B.; Goedkoop, J. B.; Hesper, R.; Pellegrin, E.; de Groot, F. M. F.; Altieri, S.; Hulbert, S. L.; Shekel, E.; Sawatzky, G. A.: Local electronic and magnetic structure of Ni below and above T_C: A spin-resolved circularly polarized resonant photoemission study. Phys. Rev. Lett. **79** (1997) 3510–3513.
[110] Kreutz, T. J.; Greber, T.; Aebi, P.; Osterwalder, J.: Temperature-dependent electronic structure of nickel metal. Phys. Rev. B **58** (1989) 1300-1317.
[111] Savrasov, S. Y.; Kotliar, G.: Linear response calculations of lattice dynamics in strongly correlated systems. Phys. Rev. Lett. **90** (2003) 056401-056404.
[112] Savrasov, S. Y.; Kotliar, G.; Abrahams, E.: Correlated electrons in δ-plutonium within a dynamical mean-field picture. Nature **410** (2001) 793-795.
[113] Dai, X.; Savrasov, S. Y.; Kotliar, G.; Migliori, A.; Ledbetter, H.; Abrahams, E.: Calculated phonon spectra of Plutonium at high temperatures. Science **300** (2003) 953-955.
[114] For a review, see e.g.: The Actinides: Electronic Strucuture and Related Properties (Eds. A. J. Freeman and J. B. Darby), Vols. 1 and 2. Academic Press, New York, 1974.
[115] Hecker, S. S.; Timofeeva, L. F.: A tale of two diagrams. Los Alamos Science **26** (2000) 244-251.
[116] Boring, A. M.; Smith, J. L.: Plutonium Condensed Matter physics – A Survey of Theory and Experiment. Los Alamos Science **26** (2000) 90-127.
[117] Arko, A. J.; Joyce, J. J.; Morales, L.; Wills, J.; Jashley, J.: Electronic structure of *alpha* - and *delta* -Pu from photoelectron spectroscopy. Phys. Rev. B **62** (2000) 1773-1779.
[118] Solovyev, I. V.; Liechtenstein, A. I.; Gubanov, V. A.; Antropov, V. P.; Andersen, O. K.: Spin-polarized relativistic linear-muffin-tin-orbital method: Volume-dependent electronic structure and magnetic moment of plutonium. Phys. Rev. B **43** (1991) 14414—14422.
[119] For recent calculations, see: Söderlind, P.; Eriksson, O.; Johansson, B.; Wills, J. M.: Electronic properties of f-electron metals using the generalized gradient approximation. Phys. Rev. B **50** (1994) 7291–7294; M. D. Jones, J. C. Boettger, R. C. Albers, and D. J. Singh, Phys. Rev. B**61**, 4644 (2000).
[120] Savrasov, S. Y.; Kotliar, G.: Ground State Theory of *delta* -Pu. Phys. Rev. Lett. **84** (2000) 3670–3673; Bouchet J, Siberchicot B., Jollet F., Equilibrium properties of delta-Pu: LDA+U calculations, Journal of Physics: Condensed Matter, **12**, (2000) 1723-1733.
[121] Söderlind, P.: Ambient pressure phase diagram of plutonium: A unified theory for α-Pu and δ-Pu. Europhys. Lett. **55** (2001) 525-531.
[122] Eriksson, O.; Becker, J. D.; Balatsky, A. V.; Wills, J. M.: Novel electronic configuration in δ-Pu. J. Alloys and Comp. **287** (1999) 1-5.
[123] Petit, L.; Svane, A.; Temmerman, W. M.; Szotek, Z.: Valencies in actinides. Solid State Commun. **116** (2000) 379-383; Setty, A.; Cooper, B. R.: Electronic structure, phase transitions and diffusive properties of elemental plutonium. In *Bulletin of March Meeting of American Physical Society* (2003), abstract G15.007.
[124] Harrison, W.: p, d and f bonds in elemental solids. Phil. Mag. B **82** (2002) 1755-1766.